The cell-end marker TeaA and the microtubule polymerase AlpA contribute to microtubule guidance at the hyphal tip cortex of *Aspergillus nidulans* to provide polarity maintenance

Norio Takeshita[1,*], Daniel Mania[1], Saturnino Herrero[1], Yuji Ishitsuka[2], G. Ulrich Nienhaus[2,3,4], Marija Podolski[5,‡], Jonathon Howard[5,‡] and Reinhard Fischer[1]

[1]Karlsruhe Institute of Technology, Department of Microbiology, Hertzstrasse 16, 76187 Karlsruhe, Germany
[2]Karlsruhe Institute of Technology, Institute of Applied Physics and Center for Functional Nanostructures, Wolfgang-Gaede-Strasse 1, 76131 Karlsruhe, Germany
[3]Karlsruhe Institute of Technology, Institute of Toxicology and Genetics, Hermann-von-Helmholtz-Platz 1, 76344 Eggenstein-Leopoldshafen, Germany
[4]University of Illinois at Urbana-Champaign, Department of Physics, 1110 West Green Street, Urbana, IL 61801, USA
[5]Max Planck Institute of Molecular Cell Biology and Genetics, Pfotenhauerstrasse 108, 01307 Dresden, Germany

*Author for correspondence (norio.takeshita@KIT.edu)
‡Present address: Yale University, Department of Molecular Biophysics and Biochemistry, 266 Whitney Avenue, New Haven, CT 06511-8902, USA

Accepted 6 September 2013
Journal of Cell Science 126, 5400–5411

doi: 10.1242/jcs.129841

Summary

In the absence of landmark proteins, hyphae of *Aspergillus nidulans* lose their direction of growth and show a zigzag growth pattern. Here, we show that the cell-end marker protein TeaA is important for localizing the growth machinery at hyphal tips. The central position of TeaA at the tip correlated with the convergence of the microtubule (MT) ends to a single point. Conversely, in the absence of TeaA, the MTs often failed to converge to a single point at the cortex. Further analysis suggested a functional connection between TeaA and AlpA (an ortholog of the MT polymerase Dis1/CKAP5/XMAP215) for proper regulation of MT growth at hyphal tips. AlpA localized at MT plus-ends, and bimolecular fluorescence complementation assays suggested that it interacted with TeaA after MT plus-ends reached the tip cortex. *In vitro* MT polymerization assays showed that AlpA promoted MT growth up to sevenfold. Addition of the C-terminal region of TeaA increased the catastrophe frequency of the MTs. Thus, the control of the AlpA activity through TeaA might be a novel principle for MT growth regulation after reaching the cortex. In addition, we present evidence that the curvature of hyphal tips also could be involved in the control of MT growth at hyphal tips.

Key words: TeaA, AlpA, Polarity, Microtubule, Cell-end marker, XMAP215, *Aspergillus nidulans*, Hyphal tip

Introduction

Cell polarity is essential for the proper functioning of many cell types. During the cellular morphogenesis – from fission yeast to human cells – microtubules (MTs) deliver positional information to the proper site of cortical polarity (Li and Gundersen, 2008; Siegrist and Doe, 2007). For example, the polarization of the actin cytoskeleton and signal transduction cascades, and continuous membrane transport towards the growth site depend on MTs. To fulfill their role, MTs have to recognize a specific site at the cortex and stop elongation once they reach the cortex. MT plus-end-tracking proteins (+TIPs) play a crucial role in this. They regulate MT plus-end dynamics of polymerization and depolymerization, mediate attachment of MTs to the cell cortex, and, especially in higher eukaryotic cells, promote MT stabilization following the attachment (Akhmanova and Steinmetz, 2010; Xiang, 2006). If the concentration of α- and β-tubulin dimers is above a certain threshold, MTs polymerize *in vitro* at their plus ends in a concentration-dependent manner. However, fast MT growth *in vivo* depends on MT-associated proteins (Al-Bassam and Chang, 2011; Howard and Hyman, 2007; Howard and Hyman, 2009). For example, an MT-associated protein, XMAP215 (known as Dis1 and Alp14 in fission yeast, CKAP5 in mammals), acts as a MT polymerase and catalyzes the addition of tubulin dimers to the growing plus end (Brouhard et al., 2008; Gard and Kirschner, 1987; Kerssemakers et al., 2006; Vasquez et al., 1994). Although much work has been done to investigate the elongation stage of MT polymerization, the molecular mechanism and the role that MT polymerases play after MT plus-ends contact the cortex are only poorly understood.

Because MT dynamics and many MT functions are conserved among eukaryotes, lower eukaryotes can serve as excellent models. In *Schizosaccharomyces pombe*, the kelch-repeat protein Tea1 (tip elongation aberrant) is delivered by growing MTs to the cell ends (Mata and Nurse, 1997). Tea1 reaches the MT plus end by the action of the kinesin-7, Tea2 (Browning et al., 2003; Browning et al., 2000), and is anchored at the cell-end membrane through the interaction with the prenylated protein Mod5 (Snaith and Sawin, 2003). At the cell end, Tea1 interacts with additional

components, which ultimately recruit the formin For3 (Feierbach et al., 2004; Martin and Chang, 2003; Tatebe et al., 2008). For3 mediates the formation of actin cables required for exocytosis for polarized growth. Tea1 (one of the cell-end markers) thus transmits positional information regulated by MTs to the actin cytoskeleton and thereby contributes to polarized growth.

The molecular mechanism by which MTs regulate polarity maintenance is principally conserved from *S. pombe* to the filamentous fungus *Aspergillus nidulans* (Fischer et al., 2008; Higashitsuji et al., 2009; Takeshita and Fischer, 2011; Takeshita et al., 2008). Tea1 and Tea2 are conserved in *A. nidulans* as TeaA (Tea1) and KipA (Tea2), respectively (Konzack et al., 2005; Takeshita et al., 2008). Although the Mod5 sequence is not conserved in filamentous fungi, a functional counterpart, TeaR, has been discovered in *A. nidulans* (Takeshita et al., 2008). TeaA is conserved in Ascomycetes and some Basidiomycetes, such as *Cryptococcus neoformans* and *Puccinia graminis*, but not in Zygomycete. TeaR is generally conserved in Ascomycetes except in Hemiascomycetes. The *A. nidulans kipA*, *teaA* and *teaR* mutants show defects in polarity maintenance, which leads to curved (Δ*kipA* or Δ*teaR*) or zigzag growing hyphae (Δ*teaA*). The two cell-end markers TeaA and TeaR localize at hyphal tips interdependently. TeaA is delivered to hyphal tips by growing MTs (Takeshita and Fischer, 2011) and anchored to the hyphal tip cortex though the interaction with TeaR (Takeshita et al., 2008). TeaA, along with TeaC, recruits the formin, SepA, to the growth zone (Higashitsuji et al., 2009). The conserved mechanism to transmit positional information from MTs to the actin cytoskeleton is required for maintenance of polarity and the growth direction of hyphae.

Besides this role, interphase MTs have additional functions in filamentous fungi, such as distribution of nuclear and other organelles and the movement of early endosomes, thus they are important for rapid hyphal growth (Egan et al., 2012; Horio and Oakley, 2005; Peñalva, 2010; Riquelme et al., 2011; Steinberg, 2011; Xiang and Fischer, 2004; Zekert and Fischer, 2009). Interestingly, they are not essential for spore germination itself, but only for site selection of germination (Oakley and Morris, 1980; Takeshita and Fischer, 2011). Here, we analyzed the dynamic behavior of MTs at hyphal tip cortex and revealed a new role of TeaA on the regulation of MT growth.

Results

TeaA is important for localizing the growth machinery at hyphal tips

Hyphal tip growth strictly depends on a properly organized actin cytoskeleton, which is thought to facilitate the continuous flow of vesicles to the cortex and their fusion with the membrane (Berepiki et al., 2011; Taheri-Talesh et al., 2008; Taheri-Talesh et al., 2012). To investigate how TeaA determines the localization of the growth machinery at hyphal tips, we analyzed the localization of SepA, the only formin in *A. nidulans* (Sharpless and Harris, 2002). In wild type, SepA–GFP localized at the hyphal tip cortex in a crescent shape and a dot-like structure at the apex (Fig. 1A) (Harris et al., 2005). In the *teaA*-deletion strain, SepA–GFP localized at hyphal tips; however, the dot-like structure was less stable and changed between a clear dot-like and a fuzzy appearance (Fig. 1B). The dot-like structure was often displaced to one side of the tip center (Fig. 1C,D). This mislocalization of SepA–GFP appeared to precede a new growth direction (Fig. 1B, arrowheads; supplementary material Fig. S1A).

Vesicles accumulate at the hyphal tip in a structure called the Spitzenkörper (Grove and Bracker, 1970; Harris et al., 2005). Thus, labeling of proteins associated with secretory vesicles, such as the v-SNARE protein SynA, result in the labeling of the Spitzenkörper (Taheri-Talesh et al., 2008) (supplementary material Fig. S1B). Because secretory vesicles are thought to be transported to the tip membrane along actin cables by class V myosin (Taheri-Talesh et al., 2012; Zhang et al., 2011), the localization of the Spitzenkörper should correlate with that of SepA because this protein mediates the formation of the actin cables. To test this, we analyzed the localization of SynA. Although GFP–SynA in wild-type strains remained rather stable near the center of the tip, it oscillated and often moved away from

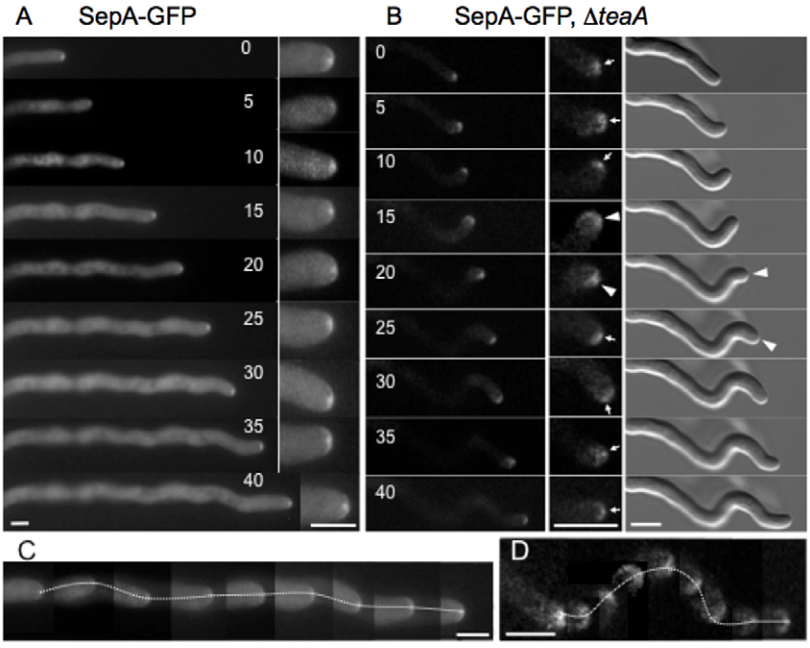

Fig. 1. Formin SepA localization at growing hyphal tips. A wild-type (A) or Δ*teaA* strain (B) expressing GFP-tagged SepA grown in minimal medium at room temperature. The elapsed time is given in minutes. (C,D) The images of hyphal tips are combined from A and B, respectively. The positions of SepA are traced by a dotted line. Scale bars: 5 μm.

the center in the tip of the *teaA*-deletion strain (supplementary material Fig. S1C). Similar to formin, the Spitzenkörper was mobile at hyphal tips and guided the growth direction of the hyphae (arrowheads). These results indicate that TeaA is important for localizing the growth machinery, such as the formin SepA and concomitantly the Spitzenkörper.

Convergence of microtubule plus-ends at the hyphal apex is mediated by TeaA

The role of MTs to transmit positional information through cell-end markers to the growth machinery is conserved in *S. pombe* and *A. nidulans*. The Spitzenkörper, however, is observed in tips of filamentous fungi but not at the cell ends of fission yeast. One reason why a Spitzenkörper is visible in filamentous fungi but not in fission yeast could be that the cell-end markers concentrate at the apex of hyphae in filamentous fungi, whereas the cell-end markers localize at multiple sites along cell ends in fission yeast (Dodgson et al., 2013). Why are cell-end markers concentrated at the apex of hyphae in *A. nidulans*? The interdependence and positive-feedback loop of TeaA and TeaR could account for this, but is apparently not sufficient because this mechanism is conserved in *S. pombe* (Snaith and Sawin, 2003; Takeshita et al., 2008). Our previous study showed that MTs in wild-type *A. nidulans* elongate toward the tips and tend to converge in the apical region where TeaA is concentrated (supplementary material Fig. S2A) (Takeshita et al., 2008). This is not observed in *S. pombe* and thus this difference could also contribute to the concentration of cell-end markers in one point in *A. nidulans*. To test this hypothesis, we analyzed the dynamic behavior of MTs at hyphal tips in more detail.

During monitoring of MT filaments, it was sometimes difficult to distinguish whether the MT plus-ends are in or out of focus. Therefore, the dynamic behavior of the kinesin-7 KipA was analyzed as an MT plus-end marker (Fig. 2A). In order to obtain quantitative data, the apical membrane, where MT plus-ends attach, was divided into a central region (0.5 µm) and side regions (Fig. 2C). GFP–KipA accumulated at MT plus-ends, moved to the hyphal tips and converged in the apical region (90%, $n=50$ in 15 hyphal tips) (supplementary material Movie 1). Interestingly TeaA seemed to play a role in the convergence of MT plus-ends, because MTs in the *teaA*-deletion strain appeared to reach the membrane more often off the center of the apex (supplementary material Fig. S2B) (Takeshita et al., 2008). In the *teaA*-deletion strain, GFP–KipA often did not merge in the apical region, but attached to several sites along the apex (Fig. 2B, 46%, $n=50$ in 20 hyphal tips) (supplementary material Movie 2). A similar pattern was observed in the same analysis using GFP-labeled MTs (Fig. 2C). These data strengthen the previous report that TeaA is necessary for the concentrated anchoring of MT plus-ends at the hyphal apex.

Because growing MTs transport TeaA to the tips of hyphae, the convergence of MT plus-ends could also focus TeaA efficiently and thereby contribute to the concentration of cell-end markers. Moreover, we observed that growing MTs reached the TeaA signal (Fig. 2D, arrow at time 0) and pushed the TeaA cluster towards the apex of the hyphal tip (arrows at 3 and 6 seconds). Then TeaA remained at the center region, even after the MT filament depolymerized (arrow at 8 seconds). This result suggests that, if the TeaA protein complex diffuses away from the center of the tip, it can be pushed back to the central position by growing MTs. Thus, it is likely that TeaA facilitates MT convergence and MTs contribute to TeaA focusing.

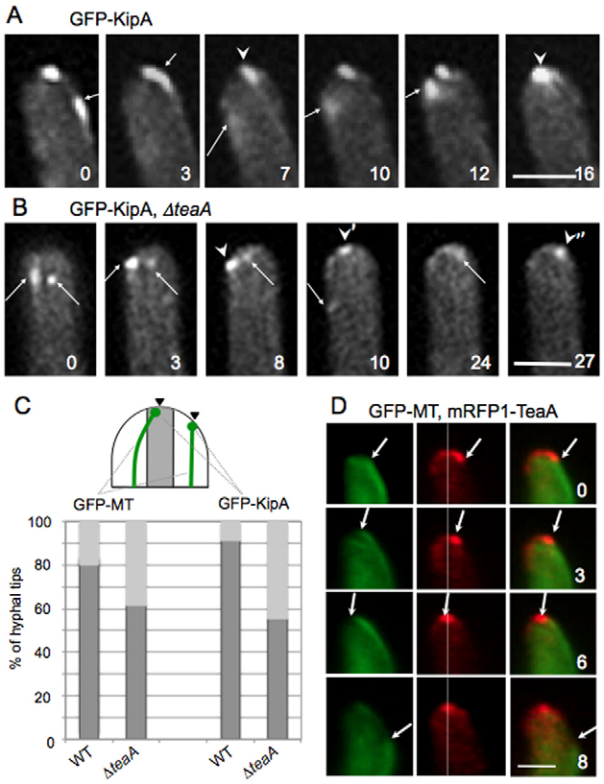

Fig. 2. Functional role of TeaA on MT dynamics at hyphal tips. (A,B) Dynamic behavior of MT plus-ends analyzed by widefield microscopy. (A) GFP–KipA accumulated at MT plus-ends (arrows) moved towards tips and reached a single point at the cortex (arrowheads). (B) GFP–KipA in the Δ*teaA* strain attached to several sites at the apex (arrowheads). (C) Quantitative analysis of the apical cortex regions where MT plus-ends are attached (GFP-labeled MTs or KipA in wild-type and Δ*teaA* strains; $n=50$ in 15–20 hyphal tips). The apical regions are classified into two parts, center (0.5 µm) or side. (D) The MT plus end (arrow at time 0) reached the TeaA cluster and then MT elongation pushed TeaA to the apex (arrows at time 3 and 6 seconds). While TeaA remained at the apex, the MT filament shrunk away (arrow in 8 seconds). The white vertical line in mRFP1–TeaA images indicates the center position of hyphal tips. The TeaA signal moved from the right side to the center with the growing MT plus end. The elapsed time is given in seconds. Scale bars: 2 µm.

Shape and curvature of hyphal tips

How is TeaA involved in the convergence of MTs? The convergence of MTs in the hyphal tip could be due to specific interactions between MT plus-end proteins and the cell-end marker protein complex (see next section). However, it could also be that the shape of the hyphal apex differs in wild-type and *teaA*-deletion strains. The tip shape would determine the angle under which MTs 'hit' the membrane, and this could regulate MT dynamics, as has been shown previously for plant cells (Dixit and Cyr, 2004) (see Discussion and supplementary material Fig. S2E).

To analyze the relationship between cell shape and MT behavior, the curvature of hyphal tips was compared between wild-type and the *teaA*-deletion strains (Fig. 3). The shape of hyphal tips was determined from analyzing hyphal tips stained

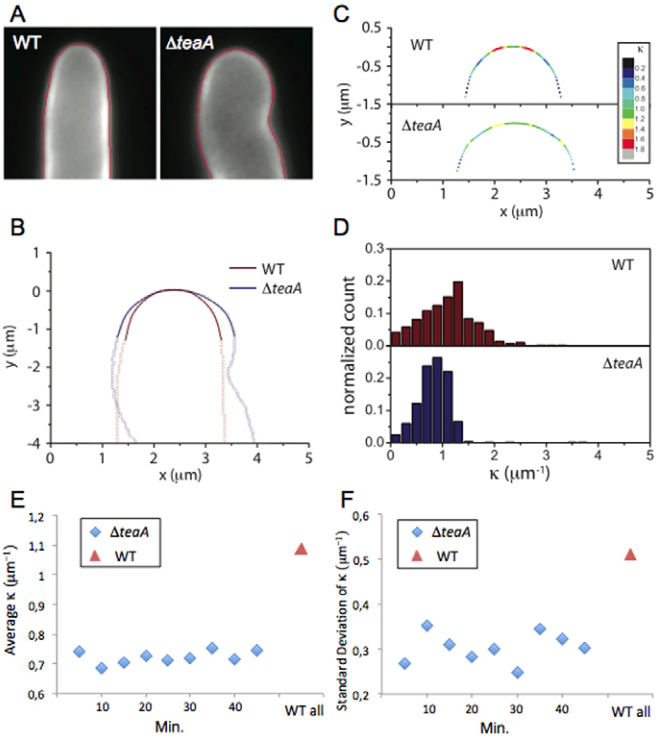

Fig. 3. Shape and curvature of hyphal tips. (A) Wild-type and Δ*teaA* strains were grown in minimal medium with glycerol at 28℃ overnight. (B) Representative segmented profiles of a wild-type (red) and a Δ*teaA* (blue) hyphal tip (open circle), and the corresponding spline fits (solid line). (C) The local curvatures have been calculated based on the spline fits in B and color-mapped onto the curve (red>blue). The color codes in C are assigned based on the local curvature, κ. The color bar on the right shows the color scale corresponding to the curvature. (D) Compiled local curvature distributions at the tips of wild-type and Δ*teaA* hyphae (n=10 each). (E,F) The averages (E) and the standard deviations (F) of curvatures (κ, in μm^{-1}) from Δ*teaA* (Fig. 1B, 0–40 minutes) and the overall average and the standard deviation of wild-type curvatures are plotted.

with Calcofluor White (Fig. 3A). Images were segmented to obtain the boundary, and its coordinates were extracted and fitted in a region 1.3 μm from the apex with a piecewise spline, from which the curvature κ was computed (see Materials and Methods) (Fig. 3B,C; supplementary material Fig. S3) (Cervantes and Tocino, 2005). The distribution of κ was broader in the wild-type strain than in the *teaA*-deletion strain (Fig. 3D, n=10 each). The results in comparison with the simulation results (supplementary material Fig. S3) indicate that the wild-type hyphal tips are more pointed (broader range of change in κ) and that the tips of the *teaA*-deletion strain are more round (more constant κ).

The average diameter of the hyphal tips at 1.3 μm from the apex was 1.8±0.2 μm for the wild-type and 2.2±0.3 μm for the *teaA*-deletion strain (±s.d., n=20 each, P=0.0001). In contrast, the diameter of subapical hyphae did not show an obvious difference between wild-type and the *teaA*-deletion strain (wild type, 2.3±0.3 μm; *teaA*-deletion strain 2.3±0.3 μm; ±s.d., n=50 each). These results also indicate that the tips of the *teaA*-deletion strain are more round than the wild-type hyphal tips (supplementary material Fig. S2E).

The shape of hyphal tips (curvature) changed during growth (Fig. 3E,F). The averages and the standard deviations of tip curvatures (κ) from the *teaA*-deletion strain (time-lapse images in Fig. 1B, 0–40 minutes) and the overall average and the standard deviation of wild-type strains are plotted (Fig. 3E,F). There were small fluctuations in both parameters; however, throughout the image sequence, the local curvature values from Δ*teaA* showed lower averages and narrower distributions in comparison to that of wild type. The result suggests that the tips of the *teaA*-deletion strain are more round than the wild-type hyphal tips independent of the growth time.

Interaction of the cell-end marker TeaA with +TIPs

To investigate the first hypothesis described above, i.e. whether a specific interaction of TeaA and MT plus-ends is involved in the convergence of MT plus-ends at the hyphal apex, the interaction of TeaA with +TIPs was screened by yeast two-hybrid analysis (supplementary material Fig. S4A). A combination of TeaA and KipA (kinesin-7) showed weak interaction. Unlike in *S. pombe*, although KipA is not necessary for TeaA accumulation at hyphal tips, it is required for correct TeaA positioning in *A. nidulans* (Takeshita et al., 2008). This is consistent with our observation of weak TeaA signals colocalizing with MT plus-ends in the *kipA*-deletion strain (supplementary material Fig. S4B,C), indicating that KipA is not essential for TeaA to localize at MT plus-ends. Interestingly, a yet undescribed positive interaction was discovered between the C-terminal half of TeaA (661–1474 aa) and the C-terminal half of AlpA (414–892 aa) (Fig. 4A,B; supplementary material Fig. S4A). AlpA is a conserved Dis1/XMAP215/CKAP5 family protein. The most conserved features of this family are N-terminal TOG domains containing multiple HEAT repeats which are known to bind tubulin from yeast to human (Al-Bassam et al., 2007; Al-Bassam et al., 2006). AlpA has a coiled-coil region at the C-terminal end, which is conserved only in fungal orthologs.

One possible role for a putative specific TeaA–AlpA interaction is to mediate their recruitment to MT plus-ends. Deletion of *alpA* markedly decreased an mRFP1–TeaA signal at hyphal tips (30% lower than the wild-type strain, supplementary material Fig. S4E) and led to mislocalization of TeaA at tips (supplementary material Fig. S4F). Deletion of *alpA* results in a drastic reduction of the MT array and dynamics (Enke et al., 2007). The mislocalization of TeaA at tips in the *alpA*-deletion strain could be a direct consequence of the reduced number of MT-mediated TeaA localization correction events due to the reduced number of MTs. Indeed, TeaA still localized at MT plus-ends even in the *alpA*-deletion strain (supplementary material Fig. S4D), indicating that AlpA is not necessary for loading or attachment of TeaA to MT plus-ends.

GFP-tagged AlpA accumulated at MT plus-ends and decorated MT filaments (Enke et al., 2007). Localization of GFP–AlpA at the MT plus-ends and along MT filaments was not strongly affected in the *teaA*-deletion strain (supplementary material Fig. S4G; Movies 3,4). These results suggest that TeaA and AlpA localize at MT plus-ends independently.

Connection between TeaA and AlpA

Further yeast two-hybrid analyses using truncated TeaA and AlpA proteins showed that the coiled-coil region of AlpA was necessary for the interaction with the C-terminal coiled-coil region of TeaA (CC3) (Fig. 4A–C). Moreover, self-interaction of the coiled-coil region of AlpA was shown, suggesting that AlpA forms homo-dimers through the coiled-coil region. Consistent with this result,

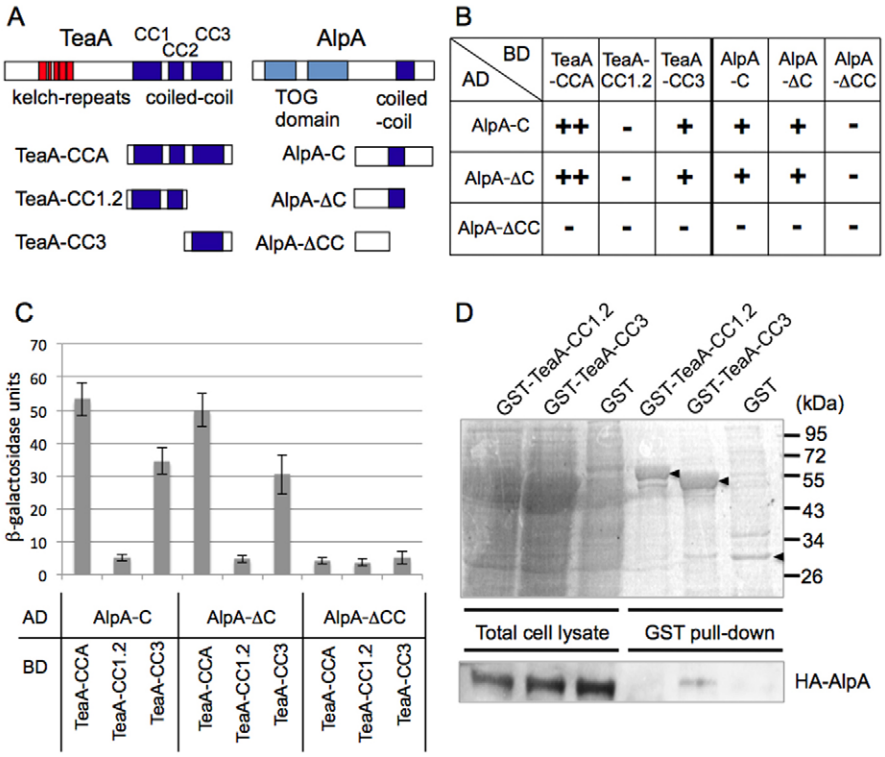

Fig. 4. Interaction between TeaA and AlpA. (A,B) Yeast two-hybrid analysis between the TeaA C-terminal and AlpA C-terminal halves. (A) A scheme of the truncated TeaA and AlpA proteins used. (B) The results of the yeast two-hybrid analysis are shown in the table. –, no interaction; +, positive interaction; ++, stronger positive interaction. (C) β-galactosidase activity was analyzed by a liquid culture assay using ONPG as substrate and is expressed as Miller units. The data are expressed as the means±s.d. of three independent experiments. (D) GST pulldown assay. An *A. nidulans* strain overexpressing HA-tagged AlpA, under the control of the *alcA* promoter, was lysed and mixed with GST only or GST-tagged TeaA-CC1.2 or TeaA-CC3 purified from *E. coli*. Glutathione–Sepharose beads were incubated with either lysate and then, after washing the beads, proteins bound to the beads were analyzed by SDS-PAGE, Coomassie Blue staining and immunoblotting with anti-HA antibody. HA–AlpA was co-immunoprecipitated with GST–TeaA-CC3.

Stu2, the XMAP215 ortholog in budding yeast, has been shown to function as a dimer through its coiled-coil region (Al-Bassam et al., 2006). Truncated AlpA lacking the coiled-coil region did not localize at MT plus-ends and did not restore the wild-type phenotype with regards to the number of MTs (supplementary material Fig. S5). Thus, the coiled-coil region is necessary for the correct localization and functioning of AlpA.

The TeaA–AlpA interaction shown in the yeast two-hybrid analysis was confirmed by GST pulldown. The cell lysate of an *A. nidulans* strain expressing HA-tagged AlpA was mixed with GST only, GST-tagged TeaA-CC1.2 (coiled-coil 1 and 2 regions of TeaA, Fig. 4A) or GST-tagged TeaA-CC3 (C-terminal coiled-coil 3 region of TeaA, Fig. 4A) purified from *E. coli* (supplementary material Fig. S6). The GST and GST-tagged proteins were precipitated with the GST-binding resin. HA–AlpA was co-precipitated with GST–TeaA-CC3 but not with GST–TeaA-CC1.2 or only GST (Fig. 4D).

To obtain spatial information about the interaction between AlpA and TeaA, bimolecular fluorescence complementation (BiFC) was used (Fig. 5A,B). When AlpA was tagged with GFP, it accumulated at MT plus-ends and moved along with them towards the hyphal tips (Fig. 6A, arrows). The signals disappeared when the MT plus-ends reached the hyphal tip (Fig. 6A, arrowheads). Next, we fused the YFP N-terminal half (YFP^N) to TeaA, and the YFP C-terminal half (YFP^C) to AlpA. In a strain expressing YFP^N–TeaA and YFP^C only, or expressing YFP^C–AlpA and YFP^N only, no YFP fluorescence was detected. In a strain expressing both YFP^N–TeaA and YFP^C–AlpA, YFP signals were clearly detected at all hyphal tips we observed (Fig. 5B, upper panels). Because AlpA localizes at MT plus-ends, and TeaA accumulates at the hyphal tip cortex, the YFP signal at hyphal tips possibly represents a connection between MT plus-ends and the hyphal tip membrane. The BiFC data suggest that there is a temporary interaction or at least close localization. However, the BiFC system is not suitable to follow the dynamics of the interaction because YFP formation is an irreversible reaction. Although both TeaA and AlpA localize at MT plus-ends, no YFP signal was detected there. This suggests that the interaction of the two proteins might be temporarily and spatially regulated. Of course, we cannot exclude that the two proteins also interact at MT plus-ends, but that the signal is too weak to be detected. In order to test the specificity of the interaction between TeaA and AlpA, we tested TeaA interaction with the other +TIPs, KipA (kinesin-7) and ClipA (a CLIP170 ortholog) (Efimov et al., 2006), containing similar coiled-coil regions. None of the combinations resulted in a positive BiFC signal (data not shown). Co-immunoprecipitation experiments using an *A. nidulans* strain producing GFP–AlpA and TeaA–HA were negative (data not shown). This might be due to the transient nature of their interaction.

Role of the C-terminal coiled-coil region of TeaA

The yeast-two hybrid and pulldown experiments described above revealed that the C-terminal coiled-coil region of TeaA (CC3) is necessary for the interaction with the coiled-coil region of AlpA. Further functional importance of this coiled-coil region in TeaA was investigated by expressing truncated TeaA versions in a *teaA*-deletion background (Fig. 5A,C–E). In addition, BiFC analyses between AlpA and the truncated TeaA versions were performed (Fig. 5A,B). Whereas wild-type TeaA tagged with mRFP1 localized at hyphal tips, neither TeaA lacking the C-terminal half (TeaAΔCC) nor lacking the coiled-coil regions CC1 and CC2 (TeaAΔCC1.2) localized at hyphal tips and they were not able to complement the phenotype of zigzag hyphae in a *teaA*-deletion strain (data not shown). The BiFC assay did not show a YFP signal in the case of the truncated TeaA proteins (TeaAΔCC and TeaAΔCC1.2, data not shown).

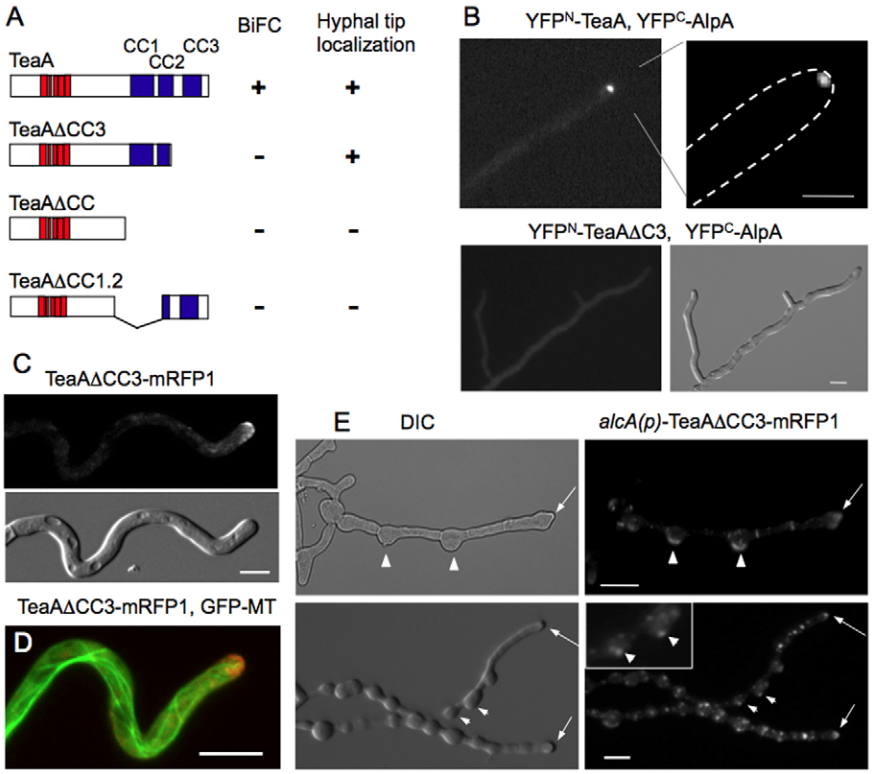

Fig. 5. Role of C-terminal coiled-coil region of TeaA (CC3). (A) Functional analysis of truncated TeaA *in vivo*. Scheme of TeaA deletions and results of localization and BiFC analysis. (B) BiFC analysis of TeaA and AlpA. In the strain expressing TeaA tagged with the N-terminal half of YFP (YFP^N) and AlpA tagged with the C-terminal half of YFP (YFP^C), the YFP signal was detected at the tip (upper panels). In the strain expressing TeaAΔCC3 tagged with YFP^N and AlpA tagged with YFP^C, the YFP signal was not detected at the tips (lower panels). (C–E) Phenotype of the strain expressing TeaAΔCC3–mRFP1 under the endogenous promoter in the *teaA*-deletion background. TeaAΔCC3–mRFP1 localized along hyphal tip cortex (C,D). (E) Phenotype of strain expressing TeaAΔCC3–mRFP1 under the control of the *alcA* promoter in the *teaA*-deletion background. TeaAΔCC3–mRFP1 localized at hyphal tip (arrows) but the strain often formed abnormal swellings along the hyphae, giving them a pearl chain appearance. TeaAΔCC3–mRFP1 localized at each swelling (arrowheads). Scale bars: 2 μm (B), 5 μm (C,E), 10 μm (D).

Interestingly, TeaAΔCC3–mRFP1 (TeaA lacking the C-terminal coiled-coil region), when expressed under an endogenous promoter in the *teaA*-deletion background, localized at hyphal tips but did not complement the zigzag phenotype of the *teaA* deletion (Fig. 5C). TeaAΔCC3–mRFP1 also did not concentrate to one point at the apex but localized widely along the hyphal tip cortex (Fig. 5C). The hyphae were wider than those of wild type (wild type 2.3±0.3 μm, TeaAΔCC3 strain 3.5±0.5 μm; ± SD, n=50 each). Although TeaAΔCC3–mRFP1 localized at hyphal tips, the BiFC assay of TeaAΔCC3 with AlpA did not show a YFP signal at tips of hyphae (Fig. 5B, lower panels). These data indicate that the CC3 region of TeaA is not necessary for the hyphal tip localization of TeaA, but is required for the proper function and the interaction with AlpA at hyphal tips.

The functional importance of the C-terminal coiled-coil region of TeaA was also shown in overexpression experiments. A strain producing TeaAΔCC3 in the *teaA*-deletion background under the control of the inducible *alcA* promoter often formed thicker hyphae and abnormal swellings along the hyphae when grown under de-repressing conditions (glycerol as the carbon source) (Fig. 5E). That phenotype was not observed in a strain producing full-length TeaA–mRFP1 under the same conditions. TeaAΔCC3–mRFP1 localized at all hyphal tips (arrows) and hyphal swellings (arrowheads). These results suggest that mislocalization of truncated TeaA induces abnormal growth at wrong places, and that the C-terminal coiled-coil region is important for polarity regulation.

Behavior of MTs in *alpA*- or *teaA*-deletion strains

In the *alpA*-deletion strain, only one or two thick MT filaments were observed in one hyphal compartment between two septa or between the hyphal tip and the first septum (Enke et al., 2007). In addition, the previous report showed that the growth of MTs only occurred occasionally, and most MTs did not elongate nor shrink in the *alpA*-deletion strain (Enke et al., 2007). To visualize the growth speed of MTs more carefully in the *alpA*-deletion strain, the movement of MT plus-ends was analyzed by kymographs using GFP–KipA as a marker (Fig. 6B,C). In comparison to wild type (Fig. 6B), GFP–KipA usually did not show any dynamic behavior (Fig. 6C, left kymograph) in the absence of AlpA within the same time interval. The rare event of GFP–KipA movement in the *alpA*-deletion strain is shown in the right kymograph of Fig. 6C. The growth rate of MTs in wild-type strains was 13.2±3.4 μm per minute (n=45 in 22 hyphae, mean±s.d.), whereas the occasional growth rate of MTs in the *alpA*-deletion strain was 4.2±1.3 μm per minute (n=7 in six hyphae, mean±s.d.). These results are consistent with our previous report (Enke et al., 2007) and confirm that the dynamic growth of MTs strongly depends on AlpA, suggesting that AlpA might function as MT polymerase (see below). We could not rule out the possibility that GFP–KipA aggregated at unknown sites in addition to MT plus-ends in the *alpA*-deletion strain, and the mechanism of how the AlpA-independent and static MTs are organized is not yet clear. If all GFP–KipA signals represent MT plus-ends, given that the number of MT plus-ends was comparable in wild type and the *alpA*-deletion strain, the static MTs possibly consist of a bundle of parallel and anti-parallel MT filaments. The occasionally observed growth of MTs might be due to a sliding of MT filaments inside of the MT bundle rather than true growth.

MTs in the *teaA*-deletion strain showed a defect in the convergence of plus ends at the apex of hyphal tips and more often reached sites at the tip cortex but off the center (Fig. 2A–C;

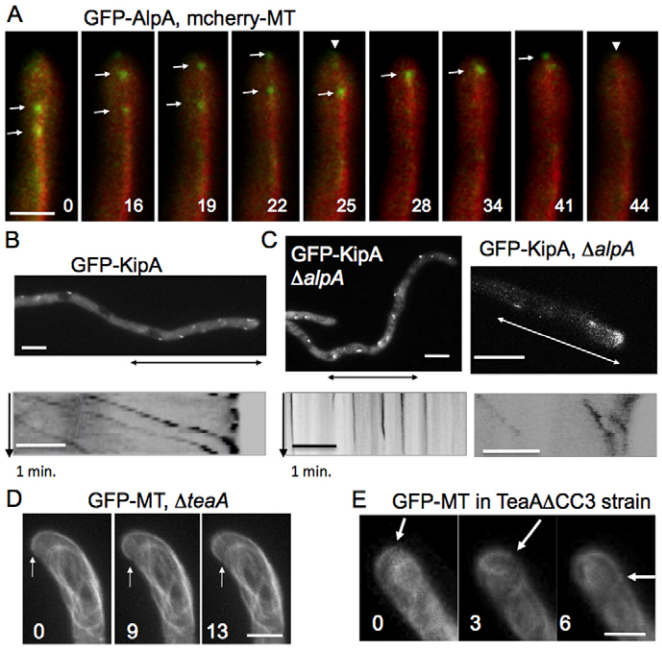

Fig. 6. Behavior of MTs in an *alpA*- or *teaA*-deletion strains. (A) GFP–AlpA localized at MT plus-ends (arrows). MTs are visualized by mCherry-tagged α-tubulin. GFP–AlpA moved towards hyphal tips as MTs elongated, then the AlpA signals disappeared when MT plus-ends reached the hyphal tip cortex. The elapsed time is given in seconds. (B,C) GFP–KipA accumulated at the MT plus-ends in wild-type (B) and in the *alpA*-deletion strain (C). Kymographs were made on segmented lines (not shown) along the hyphae restricted by the arrowed lines in wild-type (B) and in the *alpA*-deletion strain (C). The vertical arrows represent 1 minute. (D) In the Δ*teaA* strain, MTs occasionally curved around the apex of the tips. Arrows indicate MT plus-ends curving along the tip cortex. (E) The strain expressing TeaAΔCC3–mRFP1 instead of native TeaA also showed MTs curving along the tip cortex. Elapsed time is given in seconds. Scale bars: 2 μm (A,D,E), 5 μm (B,C).

supplementary material Fig. S2A,B) (Takeshita et al., 2008). MTs in the wild type grew towards hyphal tips, reached the cortex, and then immediately started to shrink. MTs in the *teaA*-deletion strain, however, sometimes reached the tip cortex and the plus ends stayed at the tips without shrinkage (10–30 seconds). Moreover, bent and curved MTs were often observed in the *teaA*-deletion strain (Takeshita et al., 2008). Additionally, in a few cases, MTs in the *teaA*-deletion strain continued to grow along the membrane of the tip cortex (Fig. 6D). This MT behavior in the *teaA*-deletion strain might suggest that TeaA is involved in the altered growth regulation of MTs at the hyphal tip cortex. A similar phenotype of MTs curling along the membrane of the tip cortex was observed in the strain expressing TeaAΔCC3 instead of TeaA (Fig. 6E).

Inspired by the yeast two-hybrid and BiFC data described above, we hypothesized that the C-terminal region of TeaA regulates termination of MT growth through the interaction with AlpA at MT plus-ends. The postulated mechanism has the potential to fine-tune MT growth at the tip cortex. To test this hypothesis, we performed an *in vitro* MT polymerization assay.

In vitro MT polymerization activity of AlpA

To investigate the function of AlpA as a MT polymerase, we used an *in vitro* MT polymerization assay with purified tubulin from porcine brains and recombinant AlpA from *E. coli* (see Materials and Methods and supplementary material Fig. S6). We used a total-internal-reflection fluorescence (TIRF) microscope to visualize MT growth. The evanescent field excitation used in a TIRF microscope restricts the excitation to only a thin sheet near the cover glass surface, minimizing the background fluorescence from free tubulin monomers that can obscure the detection of growing MTs. Surface-immobilized anti-Rhodamine antibodies were used to selectively adhere to Rhodamine-labeled MT seeds, stabilized with the non-hydrolyzable GTP analog GMPCPP, on the surface of the cover glass. When a reaction mix containing 10 μM of Alexa-Fluor-488-labeled tubulin was perfused into the chamber, MTs grew by extension (green) from the stable MT seeds (red) (Fig. 7A). Kymographs shown in Fig. 7A show MT growth and shrinkage from both ends. We judged the orientation of plus or minus ends from the growth speed at each end. At 10 μM tubulin (bulk concentration), AlpA promoted MT growth speed at plus ends in a concentration-dependent manner up to 100 nM (Fig. 7A,B; supplementary material Movie 5; Fig. S6). Given that the growth speed was not significantly enhanced at concentrations above 100 nM, this concentration was used in the following experiments. The MT growth speed in the presence of 100 nM AlpA was 6.3±0.2 μm/minute (mean±s.e.m., n=50), 7.6-fold higher than without AlpA (0.83±0.03 μm/minute, mean±s.e.m., n=50). AlpA also promoted the MT growth speed at minus ends, but only by a factor of 1.9 (100 nM AlpA, 0.55±0.03 μm/minute; 0 nM AlpA, 0.29±0.02 μm/minute, mean±s.e.m., n=20).

In the presence of AlpA, MTs also grew to longer filaments than under the control condition, as judged from the MT lengths just prior to the catastrophe (Fig. 7C; supplementary material Fig. S6; Movie 5 and 6). Without AlpA, the catastrophe occurred for MT lengths below 20 μm, whereas with 100 nM AlpA, some MTs grew up to 100 μm before a catastrophe event (n=40). Additionally, AlpA increased the catastrophe frequency in a concentration-dependent manner between 0 and 100 nM concentration range (Fig. 7D). The catastrophe frequency was calculated as the number of catastrophe events divided by the total time of MT growth (in minutes). AlpA at 100 nM concentration induced catastrophe events at a threefold higher frequency than in the control without AlpA.

Effects of TeaA on MT polymerization activity of AlpA

To test the hypothesis that the C-teminal region of TeaA affects the activity of AlpA, the coiled-coil regions (TeaA-CC1.2, TeaA-CC3, and TeaA-CCA, see Fig. 4A; supplementary material Fig. S6) were tagged with GST, purified from *E. coli*, and used in the MT polymerization assay. Under conditions of different AlpA concentrations (100, 50, 0 nM), 300 nM of the coiled-coil regions of TeaA, GST-tagged coiled-coil regions of KipA (KipA-CC, see supplementary material Fig. S6) or GST only (as a control) was added to the reaction mix. Then, we measured the growth speed of MTs and the catastrophe frequency for each condition (Fig. 8A,B). With 100 nM AlpA, TeaA-CC1.2, TeaA-CC3 and TeaA-CCA decreased the growth speed (<20%) (AlpA alone, 6.3±0.2 μm/minute; AlpA + TeaA-CC1.2, 5.2±0.2 μm/minute; AlpA + TeaA-CC3, 5.1±0.2 μm/minute; AlpA + TeaA-CCA, 5.1±0.2 μm/minute, mean±s.e.m., n=40–50) (Fig. 8A). GST alone and KipA-CC had no effect on the growth speed. TeaA-CCA also increased the catastrophe frequency (22%) (Fig. 8B). With 50 nM AlpA, TeaA-CC3, TeaA-CCA and KipA-CC did not

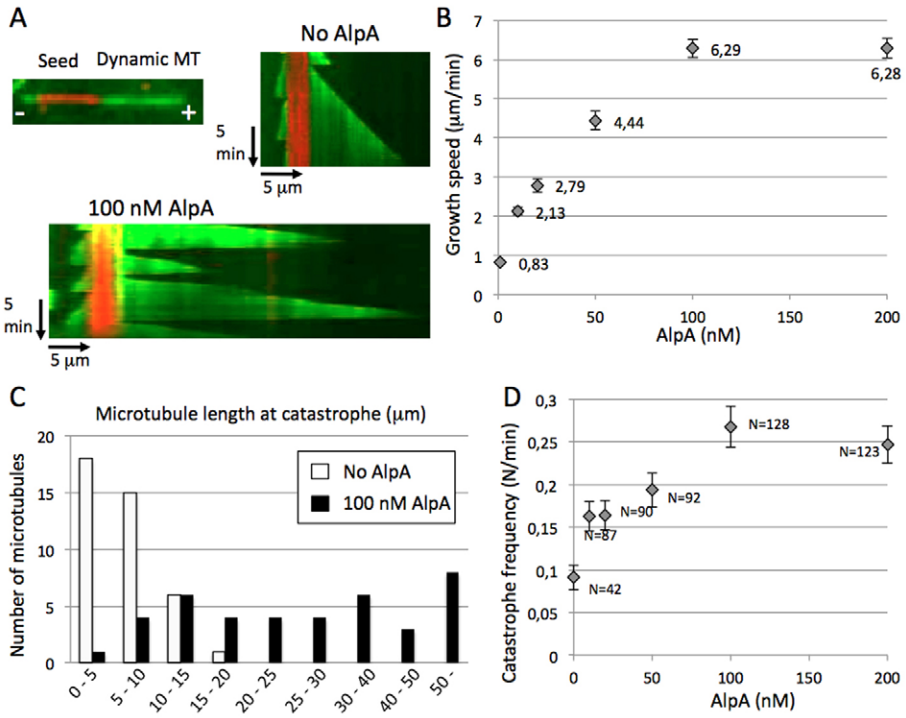

Fig. 7. *In vitro* MT polymerization assay. (A) Image of a seed MT (red) with a dynamic MT lattice growing from the plus end (green). Kymographs of MTs in the absence of AlpA (right) and presence of 100 nM AlpA (lower). (B) Plot of MT growth speed (µm/minute) against AlpA concentration. The logarithmic trendline is shown. Results are means±s.e.m. (n=50). (C) Histogram of MT length at catastrophe in the absence of AlpA (white bars) and presence of 100 nM AlpA (black bars), n=40. (D) Plot of catastrophe frequency (number of catastrophe per total time of MT growth) against AlpA concentration. Results are means±s.e.m. (the number of catastrophes counted is shown, n=42–128).

affect the growth speed. TeaA-CC3 and TeaA-CCA, however, increased the catastrophe frequency (30% and 54% respectively). In contrast, KipA-CC did not affect the catastrophe frequency. In the absence of AlpA, TeaA-CC3 and TeaA-CCA did not show obvious effects on the MT growth speed and the catastrophe frequency.

Discussion

The establishment and maintenance of cell polarity requires an interplay between the cytoskeleton and landmarks at the cortex (Li and Gundersen, 2008; Siegrist and Doe, 2007). In many cell types, MTs are polymerized from MT-organizing centers (MTOCs) located in the cytoplasm towards the cortex. An interesting and widely studied phenomenon is the control of MT-plus-end–cortex interactions and their roles for cell polarity. Our analysis shows that the cell-end marker TeaA at hyphal tips is involved in the convergence of MT plus-ends at the tip apex, and suggests that the cooperation of TeaA and the MT polymerase AlpA is important for the convergence of MTs and proper control of MT growth (supplementary material Fig. S2C,D).

Our *in vitro* analysis demonstrated that AlpA promoted MT growth in a concentration-dependent manner (up to 100 nM), resulting in a higher growth rate, longer MT filaments and a higher catastrophe frequency. The growth speed *in vitro* is comparable with that mediated by XMAP215 of *Xenopus* and ~fourfold higher than that mediated by Alp14, the XMAP215 ortholog in *S. pombe* (Al-Bassam et al., 2012; Brouhard et al., 2008). XMAP215, which functions as a monomer, contains five TOG domains, which directly bind tubulin dimers. In contrast, the fungal homologs have two TOG domains and a coiled-coil domain – probably for dimerization (Al-Bassam et al., 2006). Interestingly, it was shown that an artificial protein 'bonsai' with two TOG domains of XMAP215 and a basic region for targeting the MT lattice almost has the full polymerase activity (Widlund et al., 2011). How the mechanism of action between XMAP215 and fungal orthologs compares is an interesting open question. The rate of MT polymerization *in vivo* in *A. nidulans* leading hyphae is ~threefold higher than in *S. pombe* (Drummond and Cross, 2000; Efimov et al., 2006; Han et al., 2001), which is similar to the ratio *in vitro*. The growth speed, however, shown here *in vitro* (6.3±0.2 µm/minute) was approximately half of the growth rate determined *in vivo* (13.2±3.4 µm/minute). We do note that tubulin from porcine brains was used in our assay, as was also used for the *in vitro* XMAP215 activity determinations. However, to measure the native AlpA activity correctly and to compare the activity of XMAP215/Dis1 family proteins, tubulins will have to be purified from each organism. A new method of tubulin purification will be helpful for future studies (Widlund et al., 2012). Additionally, the AlpA activity could well be stimulated by other +TIPs, which could explain the higher MT growth rate *in vivo*.

In the absence of AlpA, the growth of MTs only occurred occasionally, and most MTs did not elongate nor shrink. The occasional growth rate of MT in the *alpA*-deletion strain was 4.2±1.3 µm/minute. The occasional growth could be the slide of the microtubule filament in microtubule bundle. We used 10 µM tubulin *in vitro*. The high concentration of tubulin induced a growth rate of 0.8 µm/minute in the absence of AlpA, however, *in vivo* the growth rate was too small to detect and this could have been because there was a lower concentration of tubulin.

Although the MT polymerase activity of AlpA was clearly shown, the inhibitory role of the C-terminal region of TeaA on the AlpA activity seemed complex. The MT growth speed in the presence of 100 nM AlpA was reduced by 20% by the C-terminal region of TeaA. Because the fast growth is AlpA concentration-dependent, the presence of TeaA fragments might bind free AlpA and block the activity. With 50 nM AlpA, TeaA-CCA increased the catastrophe frequency by 54%. The effect of TeaA-CCA was

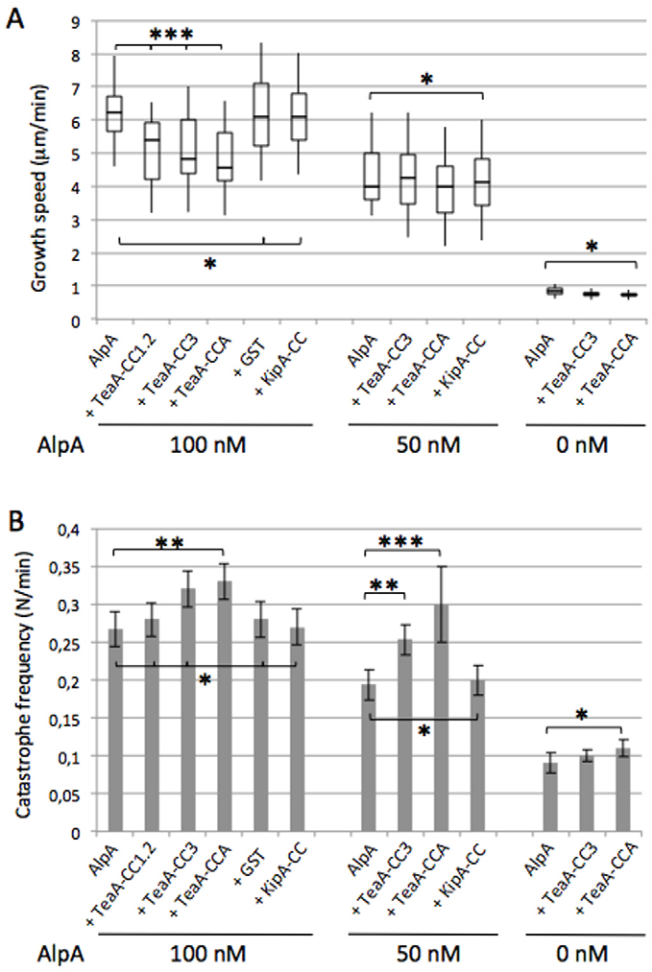

Fig. 8. Effects of TeaA on MT polymerization activity *in vitro*. (A,B) Boxplot of MT growth speed (µm/minute) (A) and bar graph of catastrophe frequency (B) at 0, 50, 100 nM AlpA with 300 nM TeaA-CC1.2, TeaA-CC3, TeaA-CCA, KipA-CC or GST. Results are means±s.e.m. (n=30–50; number of catastrophes counted, n=42–128) (B). *P>0.05 (no significant difference); **P<0.05 (statistically significant); ***P<0.001 (highly significant difference).

larger than that of TeaA-CC3, suggesting TeaA-CC1.2 is also indirectly involved in the effect although TeaA-CC1.2 alone did not show an interaction with AlpA in the yeast two-hybrid and pulldown assays. The catastrophe frequency was also dependent on the AlpA concentration. The C-terminal region of TeaA might bind AlpA at MT plus-ends, rather than free AlpA, and, hence, block its function and induce the catastrophe.

The regulation of AlpA activity *in vivo* could be more complex, because our *in vitro* system completely lacks the geometric context of the hyphal tip. At the hyphal tip, AlpA activity might be controlled directly by TeaA in addition to through the concentration of tubulin dimers. It might well be that the extensive traffic of proteins and vesicles at the tip limits the access of free tubulin dimmers, preventing them reaching the MT plus-ends. In the *in vitro* experiment, free tubulins could still come in from all directions; however, this might not be the case at the end of the cortex. As in the case of XMAP215, both forward (polymerization) and reverse (catastrophe) reactions are catalyzed by the activity of AlpA. This means that a small change in the local tubulin dimer concentration can shift the MT to favor catastrophe. Such geometric effects on the catastrophe frequency of MTs has been previously reported in other systems (Komarova et al., 2002; Janson et al., 2003). Upon reaching the membrane near the end of the hypha, MTs can either stop polymerizing immediately or, more often, can be indirectly tethered to the membrane and continue to grow until they reach the apex, where concentrated TeaA might block the AlpA activity and induce catastrophe (Fig. 2A; supplementary material Fig. S2C,D).

In our model, although both TeaA and AlpA localize at MT plus-ends, TeaA regulates the AlpA activity only at the hyphal tip. In *S. pombe*, it was speculated that the TeaA ortholog, Tea1, is phosphorylated, and that its function is regulated by the phosphorylation at different places, such as MT plus-ends and the cell-end cortex (Kim et al., 2003). If this also applies to *A. nidulans* TeaA, it is likely that the phosphorylation of TeaA is important for the interaction with AlpA and that the protein isolated from *E. coli* does not have full activity. In addition, TeaA might not be the only protein that regulates AlpA or MT growth, and its role in bringing MT plus-ends near other partnering protein could greatly contribute to allowing the downstream reactions to take place. Recently, another mechanism to regulate MT growth at the cell cortex has been revealed in fission yeast where myosin V regulates MT dynamics at the cortex, possibly through the degradation of Tip1 (one of the +TIPs, a CLIP170 ortholog) (Martín-García and Mulvihill, 2009). It appears that there are redundant pathways to fine-tune MT growth at hyphal tips.

Another possible factor that regulates MT dynamics at the cortex is the shape of hyphal tips. In plant cells, the regulation of MT growth at the cortex depends on the angle between the MTs and the cortex (Dixit and Cyr, 2004). If this angle is large enough, MTs stop elongating after the plus ends reach the cortex. In contrast, when the angle is small, MTs are able to keep growing (supplementary material Fig. S2E). Indeed, the shape of hyphal tips in the *teaA*-deletion strain was more round than in the wild type (Fig. 3). This change of the shape is probably due to unstable localization of the formin SepA and the secretory vesicle cluster in the *teaA*-deletion strain (Fig. 1B), and this in turn could further promote mislocalizations. Although the critical angle for MTs to grow or stop has not yet been revealed, the more-round tips in the *teaA*-deletion strain could explain the defects in the convergence of MTs and the curling of MTs along the tip cortex (supplementary material Fig. S2E). In a funnel-like structure, rigid MTs would automatically be centered at one point, which would not occur with a flattened tip shape. Likewise, curling of MTs along the cell end cortex has been observed in the *tea1*-deletion cells in *S. pombe*, which was remarkable in wider cells (Foethke et al., 2009). The broader hyphae or more-round hyphae might permit MTs to curl along the tip apex rather than to shrink, although the hyphae of the *teaA*-deletion strain had no obvious difference in diameter compared to wild type. Cell shape has the potential to regulate MT growth; whereas the shape is controlled by the polarity, then the polarity is controlled by the interaction between the MT plus-ends and cell cortex. The situation resembles a three-cornered-feedback loop, consisting of polarity, cell shape and MT growth (supplementary material Fig. S2G).

Growing MTs transport TeaA to hyphal tips and maintain the localization of TeaA there. At the same time, the accumulated TeaA at hyphal tips is important for the convergence of MTs.

This interdependence of TeaA and MTs could act as a positive-feedback loop to concentrate TeaA at the apex. The concentrated and well-focused polarity at the apex is probably responsible for the stable localization of both the formin SepA and accumulated secretory vesicles. The concentration of TeaA and the convergence of MTs at the apex are not observed in fission yeast and could be specifically important for the tip growth of hyphae. We proposed previously a positive-feedback model for polarized tip growth in which cell-end markers (TeaA and TeaR, their localization is interdependent), RhoGTPases (and their effectors) and sterol-rich membrane domains at tips regulate their localization interdependently (Fischer et al., 2008; Takeshita et al., 2012). The interdependence of TeaA and MTs is also thought to contribute to the process, especially to focus the polarity (supplementary material Fig. S2F) and mediate the localization and formation of the Spitzenkörper, which is not observed in fission yeast.

Moreover, the convergence of MTs at the apical region possibly determines the deposition point of secretory vesicles. At the apical region of growing hyphal tips, the Spitzenkörper (accumulation of vesicles), the exocyst complex (machinery for exocytosis), formin and the polarisome are concentrated (Grove and Bracker, 1970; Sharpless and Harris, 2002; Taheri-Talesh et al., 2008; Virag and Harris, 2006). Secretory vesicles are delivered to hyphal tips by the cooperation of actin and microtubule-dependent motors (Schuster et al., 2012; Taheri-Talesh et al., 2008; Taheri-Talesh et al., 2012; Zhang et al., 2011). If secretory vesicles need to be transferred from MTs to actin cables around the tips, the MT convergence could guarantee an effective transfer and efficient vesicle secretion. Moreover, actin cables from the tips might also be involved in MT convergence, given that the secretory vesicle has the potential to bind both MT- and actin-dependent motor proteins and, thus, to connect both tracks.

In summary, we propose a mechanism for MT convergence at the apex of hyphal tips that is a mediated by an interplay between the cell-end marker TeaA and the MT polymerase AlpA in combination with the cell shape. The convergence of MT plus-ends at polarized growth sites is thought to be important for the fine-tuning of polarity in highly polarized filamentous fungi.

Materials and Methods

Strains, plasmids and culture conditions

Supplemented minimal medium for *A. nidulans* was prepared, and standard strain construction procedures are as described previously (Hill and Käfer, 2001). A list of *A. nidulans* strains used in this study is given in supplementary material Table S1. Standard laboratory *Escherichia coli* strains (XL-1 blue, Top 10 F', BL21) were used. Plasmids are listed in supplementary material Table S2.

Molecular techniques

Standard DNA transformation procedures were used for *A. nidulans* (Yelton et al., 1984) and *E. coli* (Sambrook and Russel, 1999). For PCR experiments, standard protocols were applied using a personal Cycler (Biometra) for the reaction cycles. DNA sequencing was performed commercially (MWG Biotech, Ebersberg, Germany). DNA analyses (Southern hybridizations) were performed as described by (Sambrook and Russel, 1999).

Yeast two-hybrid analysis

The yeast two-hybrid analysis was performed using the MatchMaker3 Gal4 two-hybrid system (BD Clontech). Several plasmids and methods are as previously described (Higashitsuji et al., 2009; Takeshita et al., 2008). Fragments of *alpA* cDNA corresponding to the N-terminal half of AlpA (1–414 aa) with primers AlpA-F-*Eco*RI and AlpA-N,CDSIII, or the C-terminal half of AlpA (414–892 aa) with primers AlpA-MEF and AlpA-R-*Bam*HI, were amplified and cloned in the pGADT7 vector, which contains the GAL4 DNA-AD (activation domain) and the *LEU2* marker (BD Clontech), yielding pNT37 or pYH22. The primers used in this study are shown in supplementary material Table S3. The fragments of *alpA* cDNA from pYH22 were cloned into the pGBKT7, which contains the GAL4 DNA-BD (binding domain) and the *TRP1* marker (BD Clontech), yielding pYH25. Fragments of the C-terminal half of *alpA* without the C-terminal region (AlpA-DC, 414–756 aa) or without the C-terminal and the coiled-coil region (AlpA-DCC, 414–644 aa) were amplified with primers AlpA-MEF and AlpA-CC-*Bam*HI-rev or AlpA-bCC-*Bam*HI-rev and cloned into the pGADT7 vector, yielding pDM06 or pDM07, or into the pGBKT7 yielding, pDM08 or pDM09. Fragments of the C-terminal region of *teaA*, TeaA-CC1 (661–1127 aa), amplified with primers TeaA,C,1,F,pGBK and TeaA,C,1,R,pGBK, and TeaA-CC3 (1061–1474 aa), amplified with primers TeaA,C,3,F,pGBK and TeaA,C,3,R,pGBK, were cloned into pGBKT7 yielding, pNT39 or pNT40. pGBK7-associated plasmids were transformed into yeast Y187 (mating type *MAT*α) and pGADT7-associated plasmids were transformed into yeast AH109 (mating type *MAT*a). The system utilizes two reporter genes (*HIS3* and *LacZ*) under the control of GAL4.

Tagging with fluorescent proteins

For tagging AlpA, AlpAΔC, and AlpAΔCC with mRFP1 at the C-terminus, their DNA fragments were amplified with primers alpA-pENTR-fwd and alpA-pENTR-rev, alpA-CC-rev or alpA-bCC-AscI-rev, cloned into the entry vector pENTR/D-TOPO, and subcloned into the destination vector pMT-mRFP1 using the gateway system, yielding pMD04, pMD02 and pMD01. For tagging AlpAw/oC with mRFP1, the C-terminal region of *alpA* was amplified with primers alpA-Ct-AscI-fwd and alpA-Ct-AscI-rev and ligated with *Asc*I-digested pMD02, yielding pMD03. To investigate the function of AlpA variants, pMD01-04 were transformed in SDV86 (Δ*alpA*, GFP-MTs). Transformants were screened by microscopic analysis and the plasmid-integration events were confirmed by PCR.

For tagging TeaA, TeaAΔCC3 and TeaAΔC with mRFP1 at the C-terminus, fragments encoding TeaA, TeaAΔCC3 and TeaAΔC were amplified with primers teaA-N-for and TeaA-C1-rev or teaA-C-rev-smaI cloned into the entry vector pENTR/D-TOPO, and subcloned into the destination vector pMT-mRFP1 using the gateway system, yielding pNT19, pNT41 and pNT42. For tagging TeaAΔCC1.2 with mRFP1, the C-terminal region of *teaA* was amplified with primers teaA-C2-f-smaI and teaA-C2-rev-smaI and cloned into *Sma*I-digested pNT42, yielding pNT43. To investigate the function of TeaA variants, pNT19 and pNT41-43 were transformed into SNT80 (Δ*teaA*, GFP-MTs). Transformants were screened by microscopic analysis and single-integration events were confirmed by PCR and Southern blotting.

For the BiFC analysis, the N-terminal half of YFP (YFP^N) or the C-terminal half of YFP (YFP^C) were fused to the N-terminus of the proteins of interest. To create an N-terminal YFP^C fusion construct of AlpA, a 1.0-kb N-terminal *Asc*I–*Pac*I fragment of *alpA* (starting from ATG) from pCE08 (Enke et al., 2007) was subcloned into the corresponding sites of pDV8, yielding pYH12. To create an N-terminal YFP^C fusion construct of TeaAΔCC3, TeaAΔCC and TeaAΔCC1.2, fragments of TeaAΔCC3, TeaAΔCC and TeaAΔCC1.2 were amplified from plasmids corresponding to the mRFP1 tagging with primers BiFC-teaA-f-psiI and BiFC-teaA-N-rev-pacI, BiFC-teaA-C1-rev-pacI or BiFC-teaA-C2-re-pacI and cloned into *Psi*I–*Pac*I-digested pYH01, yielding pNT44, pNT45 and pNT46. The *alcA* promoter and YFP^N of pNT46 were replaced with the 1.5-kb *teaA* promoter, yielding pYH60 and mRFP1 from pNT28, yielding pNT50. To investigate the interaction of AlpA with TeaA, pYH12 ($alcA_{(p)}$-YFP^C-AlpA) and pYH01 ($alcA_{(p)}$-YFP^N-TeaA) or pYH60 ($teaA_{(p)}$-YFP^N-TeaA) were transformed in TN02A3. To investigate the interaction of AlpA with TeaA variants, pYH12 ($alcA_{(p)}$-YFP^C-AlpA) and pNT44-46 in which AlpA and TeaA variants were expressed under the *alcA* promoter, were transformed into the SSK91 strain (Δ*teaA*). pNT50 was transformed in SNT80 (Δ*teaA*, GFP-tagged MTs). Transformatns were screened by microscopic analysis and the integration events were confirmed by PCR.

For tagging SynA with GFP at the N-terminus, a 0.4-kb N-terminal fragment of *synA* was amplified by SynA_AscI_fwd and PacI_SynA_rev2. The *Asc*I–*Pac*I fragment of *synA* was subcloned into the corresponding sites of pMCB17apx, yielding pNG2. pNG2 was transformed into TN02A3. Transformants were screened by microscopic analysis and the single integration events were confirmed by Southern blotting.

Optical microscopy

For live-cell imaging of germlings and hyphae, cells were grown on coverslips in 0.5 ml supplemented minimal medium with 2% glucose. If a certain protein is expressed under the regulatable *alcA* promoter, supplemented minimal medium with 2% glycerol (*alcA* de-repressive condition) was used. Cells were incubated at 28℃ overnight. Coverslips were mounted on a microscope slide. For long-term live-cell imaging of SepA–GFP and GFP–SynA, glass-bottomed FluoroDishs (World Precision Instruments) were used. Tempcontrol mini (Pepcon) was used as needed to control the temperature of the specimens during the imaging. Images were captured using an Axiophot microscope equipped with a Planapochromatic 63× oil immersion objective lens, the Zeiss AxioCam MRM camera (Zeiss, Jena, Germany) and the HBO103 mercury arc lamp (Osram) or HXP 120 (Zeiss, Jena, Germany), which has a faster wavelength switching speed. Images were collected

and analyzed using the AxioVision system (Zeiss). The quantitative analysis of signal intensities and the kymograph analysis were performed by using the ImageJ software (http://rsb.info.nih.gov/ij/).

Local curvature analysis

Local curvatures, κ, of hyphal tips were determined from analyzing fluorescence images of wild-type and Δ*teaA* hyphae stained with Calcofluor White ($n=10$ each). For time-lapse analysis, DIC images were used. Each image was aligned, cropped (150×150 pixels) and smoothed by a Gaussian filter (1 pixel) using Adobe Photoshop. Images were segmented to get the outline, and its coordinates were extracted and fitted in a region 1.3 µm from the apex with a piecewise spline (7 pieces, 5th order) using a combination of a custom-written and a shared MATLAB code (SPLINEFIT). Using the obtained fitted equations, κ was computed by suing $|y''|/(1+y'2)^{3/2}$ for 100 points evenly spaced in x range (~0.02 µm spacing) (Cervantes and Tocino, 2005) (y is the function obtained from the spline fit, and y' and y'' denote the first and second derivatives of y, respectively).

Protein expression in *E. coli*

A fragment of *teaA* cDNA corresponding to the coiled-coil 1 and 2 regions of TeaA (TeaA-CC1.2; 661–1122 aa) was amplified with primers GST-TeaAC1-f-bam and GST-TeaAC1-r-eco, and the coiled-coil 3 region (TeaA-CC3; 1061–1474 aa) was amplified with primers GST-TeaAC3-f-bam and GST-TeaAC3-r-eco. The C-terminal half of TeaA (TeaA-CA; 661–1474 aa) was amplified with primers GST-TeaAC1-f-bam and GST-TeaAC3-r-eco. A fragment of *kipA* cDNA corresponding to the coiled-coil region of KipA (KipA-CC; 505–800 aa) was amplified with primers KipCC-GST-f-BmH and kipCC-GST-r-Xho. These cDNA fragments were cloned into pGEX-4T-1 (Invitrogen) for protein expression, yielding pNT53, pNT54, pNT74 and pNT73. Fragments of *alpA* cDNA (full-length 892 aa) were codon-optimized and synthesized (Genescript) and subcloned into pET-28a (Novagen). The GST-tagged TeaA C-terminal regions and the coiled-coil region of KipA and His-tagged AlpA were purified from BL21 *E. coli* grown in 200 ml culture by using GST-bound resin (Novagen) or Ni^{2+}-NTA (QIAGEN) under native conditions, according to the manufacturers' instructions. Buffers of the purified proteins were exchanged using the concentrator Vivaspin (Sartorius stedim) to BRB80 buffer (80 mM PIPES pH 6.9, 1 mM $MgCl_2$ and 1 mM EGTA) for the *in vitro* MT polymerization assay. Protein concentrations were measured using the Bradford assay (BioRad). Purification of proteins was visualized by SDS-PAGE and Coomassie Blue staining (supplementary material Fig. S6). Freshly purified proteins, 7 µM His–AlpA, 5.4 µM GST–TeaA-CC1.2, 9.1 µM GST-TeaA-CC3, 6.1 µM GST-TeaA-CA, and 9.1 µM GST-KipA-CC, were used for the *in vitro* assay.

Pulldown assay

For induction of the *alcA* promoter, *A. nidulans* SCE05 strain was cultured in minimal medium containing 2% threonine and 0.2% glucose for 24 hours. The mycelia was ground in liquid nitrogen, resuspended in protein extraction buffer (20 mM Tris-HCl pH 8, 150 mM NaCl, 0.05% Triton X-100) and centrifuged at 10,000 ***g*** at 4℃ for 10 minutes. The supernatants were incubated at 4℃ for 2 hours with or without purified C-terminal TeaA proteins from *E. coli* and then, incubated with GST-binding resin (Novagen) additional for 1 hour. The reaction mixes were centrifuged and the pellets were washed two times with protein extraction buffer and analyzed by SDS-PAGE, Coomassie Blue staining and immunoblotting with anti-HA antibodies.

In vitro MT polymerization assay

Purification of porcine brain tubulin (Ashford et al., 1998), labeling of tubulin with Alexa Fluor 488 (Hyman et al., 1991) and assay conditions (Brouhard et al., 2008; Gell et al., 2010) were as described previously. Reaction channels sandwiched by silanized cover glasses were initially filled with PBS buffer, then incubated with 1% anti-Rhodamine antibody (Invitrogen) in PBS for 5 minutes, followed by 1% pluronic F127 (Sigma) in PBS for 15 minutes and were finally filled with Rhodamine-labeled GMPCPP-stabilized MT seeds. The reaction channels were placed under the TIRF microscope. An objective heater was used to warm the sample to 35℃. A 20 µl reaction mix containing 10 µM tubulin (10% Alexa-labeled tubulin), 40 mM D-glucose, 40 µg/ml glucose oxidase, 20 µg/ml catalase, 20 mM dithiothreitol, 50 mM KCl, 1 mM GTP and AlpA (0–200 nM) or TeaA C-terminal regions (300 nM) were perfused into the reaction channels. Images were collected with an Andor DV887 iXon camera on a Zeiss Axiovert 200 M microscope using a Zeiss 100×, 1.45 NA Plan-FLUAR objective. Standard filter sets were used to visualize Alexa Fluor 488 and Rhodamine fluorescence. The integration time for each frame was 100 milliseconds. Images of time-lapse movies were taken every 10 seconds for 15 minute.

Acknowledgements

We thank Y. Higashitsuji, N. Grün and N. Bühler for technical assistance. The authors declare that they have no conflict of interest.

Author contributions

N.T. and R.F. conceived the experiments and wrote the manuscript; N.T., D.M. and S.H. performed experiments; N.T., Y.I. and G.U.N. analyzed data of curvature of hyphal tips. N.T., M.P. and J.H. analyzed data of *in vitro* MT polymerization assay.

Funding

The work was supported by the Deutsche Forschungsgemeinschaft [grant numbers TA819/2-1 to N.T. and FOR1334, Centre for Functional Nanostructures to R.F.]; and the Baden Württemberg Stiftung to N.T.

Supplementary material available online at
http://jcs.biologists.org/lookup/suppl/doi:10.1242/jcs.129841/-/DC1

References

Akhmanova, A. and Steinmetz, M. O. (2010). Microtubule +TIPs at a glance. *J. Cell Sci.* **123**, 3415-3419.

Al-Bassam, J. and Chang, F. (2011). Regulation of microtubule dynamics by TOG-domain proteins XMAP215/Dis1 and CLASP. *Trends Cell Biol.* **21**, 604-614.

Al-Bassam, J., van Breugel, M., Harrison, S. C. and Hyman, A. (2006). Stu2p binds tubulin and undergoes an open-to-closed conformational change. *J. Cell Biol.* **172**, 1009-1022.

Al-Bassam, J., Larsen, N. A., Hyman, A. A. and Harrison, S. C. (2007). Crystal structure of a TOG domain: conserved features of XMAP215/Dis1-family TOG domains and implications for tubulin binding. *Structure* **15**, 355-362.

Al-Bassam, J., Kim, H., Flor-Parra, I., Lal, N., Velji, H. and Chang, F. (2012). Fission yeast Alp14 is a dose-dependent plus end-tracking microtubule polymerase. *Mol. Biol. Cell* **23**, 2878-2890.

Ashford, A. J., Anderson, S. S. L. and Hyman, A. A. (1998). Preparation of tubulin from bovine brain. In *Cell Biology: A Laboratory Handbook.* pp. 205-212. San Diego: Academic Press.

Berepiki, A., Lichius, A. and Read, N. D. (2011). Actin organization and dynamics in filamentous fungi. *Nat. Rev. Microbiol.* **9**, 876-887.

Brouhard, G. J., Stear, J. H., Noetzel, T. L., Al-Bassam, J., Kinoshita, K., Harrison, S. C., Howard, J. and Hyman, A. A. (2008). XMAP215 is a processive microtubule polymerase. *Cell* **132**, 79-88.

Browning, H., Hayles, J., Mata, J., Aveline, L., Nurse, P. and McIntosh, J. R. (2000). Tea2p is a kinesin-like protein required to generate polarized growth in fission yeast. *J. Cell Biol.* **151**, 15-28.

Browning, H., Hackney, D. D. and Nurse, P. (2003). Targeted movement of cell end factors in fission yeast. *Nat. Cell Biol.* **5**, 812-818.

Cervantes, E. and Tocino, A. (2005). Geometric analysis of Arabidopsis root apex reveals a new aspect of the ethylene signal transduction pathway in development. *J. Plant Physiol.* **162**, 1038-1045.

Dixit, R. and Cyr, R. (2004). Encounters between dynamic cortical microtubules promote ordering of the cortical array through angle-dependent modifications of microtubule behavior. *Plant Cell* **16**, 3274-3284.

Dodgson, J., Chessel, A., Yamamoto, M., Vaggi, F., Cox, S., Rosten, E., Albrecht, D., Geymonat, M., Csikasz-Nagy, A., Sato, M. et al. (2013) Spatial segregation of polarity factors into distinct cortical clusters is required for cell polarity control. *Nat. Commun.* **4**, 1834.

Drummond, D. R. and Cross, R. A. (2000). Dynamics of interphase microtubules in Schizosaccharomyces pombe. *Curr. Biol.* **10**, 766-775.

Efimov, V. P., Zhang, J. and Xiang, X. (2006). CLIP-170 homologue and NUDE play overlapping roles in NUDF localization in *Aspergillus nidulans. Mol. Biol. Cell* **17**, 2021-2034.

Egan, M. J., McClintock, M. A. and Reck-Peterson, S. L. (2012). Microtubule-based transport in filamentous fungi. *Curr. Opin. Microbiol.* **15**, 637-645.

Enke, C., Zekert, N., Veith, D., Schaaf, C., Konzack, S. and Fischer, R. (2007). *Aspergillus nidulans* Dis1/XMAP215 protein AlpA localizes to spindle pole bodies and microtubule plus ends and contributes to growth directionality. *Eukaryot. Cell* **6**, 555-562.

Feierbach, B., Verde, F. and Chang, F. (2004). Regulation of a formin complex by the microtubule plus end protein tea1p. *J. Cell Biol.* **165**, 697-707.

Fischer, R., Zekert, N. and Takeshita, N. (2008). Polarized growth in fungi—interplay between the cytoskeleton, positional markers and membrane domains. *Mol. Microbiol.* **68**, 813-826.

Foethke, D., Makushok, T., Brunner, D. and Nédélec, F. (2009). Force- and length-dependent catastrophe activities explain interphase microtubule organization in fission yeast. *Mol. Syst. Biol.* **5**, 241.

Gard, D. L. and Kirschner, M. W. (1987). A microtubule-associated protein from Xenopus eggs that specifically promotes assembly at the plus-end. *J. Cell Biol.* **105**, 2203-2215.

Gell, C., Bormuth, V., Brouhard, G. J., Cohen, D. N., Diez, S., Friel, C. T., Helenius, J., Nitzsche, B., Petzold, H., Ribbe, J. et al. (2010). Microtubule dynamics reconstituted in vitro and imaged by single-molecule fluorescence microscopy. *Methods Cell Biol.* **95**, 221-245.

Grove, S. N. and Bracker, C. E. (1970). Protoplasmic organization of hyphal tips among fungi: vesicles and Spitzenkörper. *J. Bacteriol.* **104**, 989-1009.
Han, G., Liu, B., Zhang, J., Zuo, W., Morris, N. R. and Xiang, X. (2001). The *Aspergillus* cytoplasmic dynein heavy chain and NUDF localize to microtubule ends and affect microtubule dynamics. *Curr. Biol.* **11**, 719-724.
Harris, S. D., Read, N. D., Roberson, R. W., Shaw, B., Seiler, S., Plamann, M. and Momany, M. (2005). Polarisome meets spitzenkörper: microscopy, genetics, and genomics converge. *Eukaryot. Cell* **4**, 225-229.
Herrero, S., Takeshita, N. and Fischer, R. (2011). The *Aspergillus nidulans* CENP-E kinesin motor KipA interacts with the fungal homologue of the centromere-associated protein CENP-H at the kinetochore. *Mol. Microbiol.* **80**, 981-994.
Higashitsuji, Y., Herrero, S., Takeshita, N. and Fischer, R. (2009). The cell end marker protein TeaC is involved in growth directionality and septation in *Aspergillus nidulans. Eukaryot. Cell* **8**, 957-967.
Hill, T. W. and Käfer, E. (2001). Improved protocols for *Aspergillus* minimal medium: trace element and minimal medium salt stock solutions. *Fungal Genet. Newsl.* **48**, 20-21.
Horio, T. and Oakley, B. R. (2005). The role of microtubules in rapid hyphal tip growth of *Aspergillus nidulans. Mol. Biol. Cell* **16**, 918-926.
Howard, J. and Hyman, A. A. (2007). Microtubule polymerases and depolymerases. *Curr. Opin. Cell Biol.* **19**, 31-35.
Howard, J. and Hyman, A. A. (2009). Growth, fluctuation and switching at microtubule plus ends. *Nat. Rev. Mol. Cell Biol.* **10**, 569-574.
Hyman, A., Drechsel, D., Kellogg, D., Salser, S., Sawin, K., Steffen, P., Wordeman, L. and Mitchison, T. (1991). Preparation of modified tubulins. *Methods Enzymol.* **196**, 478-485.
Janson, M. E., de Dood, M. E. and Dogterom, M. (2003). Dynamic instability of microtubules is regulated by force. *J. Cell Biol.* **161**, 1029-1034.
Karos, M. and Fischer, R. (1999). Molecular characterization of HymA, an evolutionarily highly conserved and highly expressed protein of *Aspergillus nidulans. Mol. Gen. Genet.* **260**, 510-521.
Kerssemakers, J. W., Munteanu, E. L., Laan, L., Noetzel, T. L., Janson, M. E. and Dogterom, M. (2006). Assembly dynamics of microtubules at molecular resolution. *Nature* **442**, 709-712.
Kim, H., Yang, P., Catanuto, P., Verde, F., Lai, H., Du, H., Chang, F. and Marcus, S. (2003). The kelch repeat protein, Tea1, is a potential substrate target of the p21-activated kinase, Shk1, in the fission yeast, Schizosaccharomyces pombe. *J. Biol. Chem.* **278**, 30074-30082.
Komarova, Y. A., Vorobjev, I. A. and Borisy, G. G. (2002). Life cycle of MTs: persistent growth in the cell interior, asymmetric transition frequencies and effects of the cell boundary. *J. Cell Sci.* **115**, 3527-3539.
Konzack, S., Rischitor, P. E., Enke, C. and Fischer, R. (2005). The role of the kinesin motor KipA in microtubule organization and polarized growth of *Aspergillus nidulans. Mol. Biol. Cell* **16**, 497-506.
Li, R. and Gundersen, G. G. (2008). Beyond polymer polarity: how the cytoskeleton builds a polarized cell. *Nat. Rev. Mol. Cell Biol.* **9**, 860-873.
Martin, S. G. and Chang, F. (2003). Cell polarity: a new mod(e) of anchoring. *Curr. Biol.* **13**, R711-R713.
Martín-García, R. and Mulvihill, D. P. (2009). Myosin V spatially regulates microtubule dynamics and promotes the ubiquitin-dependent degradation of the fission yeast CLIP-170 homologue, Tip1. *J. Cell Sci.* **122**, 3862-3872.
Mata, J. and Nurse, P. (1997). tea1 and the microtubular cytoskeleton are important for generating global spatial order within the fission yeast cell. *Cell* **89**, 939-949.
Nayak, T., Szewczyk, E., Oakley, C. E., Osmani, A., Ukil, L., Murray, S. L., Hynes, M. J., Osmani, S. A. and Oakley, B. R. (2006). A versatile and efficient gene-targeting system for *Aspergillus nidulans. Genetics* **172**, 1557-1566.
Oakley, B. R. and Morris, N. R. (1980). Nuclear movement is β-tubulin-dependent in *Aspergillus nidulans. Cell* **19**, 255-262.
Peñalva, M. A. (2010). Endocytosis in filamentous fungi: Cinderella gets her reward. *Curr. Opin. Microbiol.* **13**, 684-692.
Riquelme, M., Yarden, O., Bartnicki-Garcia, S., Bowman, B., Castro-Longoria, E., Free, S. J., Fleissner, A., Freitag, M., Lew, R. R., Mouriño-Pérez, R. et al. (2011). Architecture and development of the *Neurospora crassa* hypha – a model cell for polarized growth. *Fungal Biol.* **115**, 446-474.
Sambrook, J. and Russel, D. W. (1999). *Molecular Cloning: A Laboratory Manual*. Cold Spring Harbor, NY: Cold Spring Harbor Laboratory Press.
Schuster, M., Treitschke, S., Kilaru, S., Molloy, J., Harmer, N. J. and Steinberg, G. (2012). Myosin-5, kinesin-1 and myosin-17 cooperate in secretion of fungal chitin synthase. *EMBO J.* **31**, 214-227.
Sharpless, K. E. and Harris, S. D. (2002). Functional characterization and localization of the *Aspergillus nidulans* formin SEPA. *Mol. Biol. Cell* **13**, 469-479.
Siegrist, S. E. and Doe, C. Q. (2007). Microtubule-induced cortical cell polarity. *Genes Dev.* **21**, 483-496.
Snaith, H. A. and Sawin, K. E. (2003). Fission yeast mod5p regulates polarized growth through anchoring of tea1p at cell tips. *Nature* **423**, 647-651.
Steinberg, G. (2011). Motors in fungal morphogenesis: cooperation versus competition. *Curr. Opin. Microbiol.* **14**, 660-667.
Taheri-Talesh, N., Horio, T., Araujo-Bazán, L., Dou, X., Espeso, E. A., Peñalva, M. A., Osmani, S. A. and Oakley, B. R. (2008). The tip growth apparatus of *Aspergillus nidulans. Mol. Biol. Cell* **19**, 1439-1449.
Taheri-Talesh, N., Xiong, Y. and Oakley, B. R. (2012). The functions of myosin II and myosin V homologs in tip growth and septation in *Aspergillus nidulans. PLoS ONE* **7**, e31218.
Takeshita, N. and Fischer, R. (2011). On the role of microtubules, cell end markers, and septal microtubule organizing centres on site selection for polar growth in *Aspergillus nidulans. Fungal Biol.* **115**, 506-517.
Takeshita, N., Higashitsuji, Y., Konzack, S. and Fischer, R. (2008). Apical sterol-rich membranes are essential for localizing cell end markers that determine growth directionality in the filamentous fungus *Aspergillus nidulans. Mol. Biol. Cell* **19**, 339-351.
Takeshita, N., Diallinas, G. and Fischer, R. (2012). The role of flotillin FloA and stomatin StoA in the maintenance of apical sterol-rich membrane domains and polarity in the filamentous fungus *Aspergillus nidulans. Mol. Microbiol.* **83**, 1136-1152.
Tatebe, H., Nakano, K., Maximo, R. and Shiozaki, K. (2008). Pom1 DYRK regulates localization of the Rga4 GAP to ensure bipolar activation of Cdc42 in fission yeast. *Curr. Biol.* **18**, 322-330.
Toews, M. W., Warmbold, J., Konzack, S., Rischitor, P., Veith, D., Vienken, K., Vinuesa, C., Wei, H. and Fischer, R. (2004). Establishment of mRFP1 as a fluorescent marker in *Aspergillus nidulans* and construction of expression vectors for high-throughput protein tagging using recombination in vitro (GATEWAY). *Curr. Genet.* **45**, 383-389.
Vasquez, R. J., Gard, D. L. and Cassimeris, L. (1994). XMAP from *Xenopus* eggs promotes rapid plus end assembly of microtubules and rapid microtubule polymer turnover. *J. Cell Biol.* **127**, 985-993.
Virag, A. and Harris, S. D. (2006). Functional characterization of *Aspergillus nidulans* homologues of Saccharomyces cerevisiae Spa2 and Bud6. *Eukaryot. Cell* **5**, 881-895.
Widlund, P. O., Stear, J. H., Pozniakovsky, A., Zanic, M., Reber, S., Brouhard, G. J., Hyman, A. A. and Howard, J. (2011). XMAP215 polymerase activity is built by combining multiple tubulin-binding TOG domains and a basic lattice-binding region. *Proc. Natl. Acad. Sci. USA* **108**, 2741-2746.
Widlund, P. O., Podolski, M., Reber, S., Alper, J., Storch, M., Hyman, A. A., Howard, J. and Drechsel, D. N. (2012). One-step purification of assembly-competent tubulin from diverse eukaryotic sources. *Mol. Biol. Cell* **23**, 4393-4401.
Xiang, X. (2006). A +TIP for a smooth trip. *J. Cell Biol.* **172**, 651-654.
Xiang, X. and Fischer, R. (2004). Nuclear migration and positioning in filamentous fungi. *Fungal Genet. Biol.* **41**, 411-419.
Yelton, M. M., Hamer, J. E. and Timberlake, W. E. (1984). Transformation of *Aspergillus nidulans* by using a trpC plasmid. *Proc. Natl. Acad. Sci. USA* **81**, 1470-1474.
Zekert, N. and Fischer, R. (2009). The *Aspergillus nidulans* kinesin-3 UncA motor moves vesicles along a subpopulation of microtubules. *Mol. Biol. Cell* **20**, 673-684.
Zhang, J., Tan, K., Wu, X., Chen, G., Sun, J., Reck-Peterson, S. L., Hammer, J. A., III and Xiang, X. (2011). *Aspergillus* myosin-V supports polarized growth in the absence of microtubule-based transport. *PLoS ONE* **6**, e28575.

Figure S1

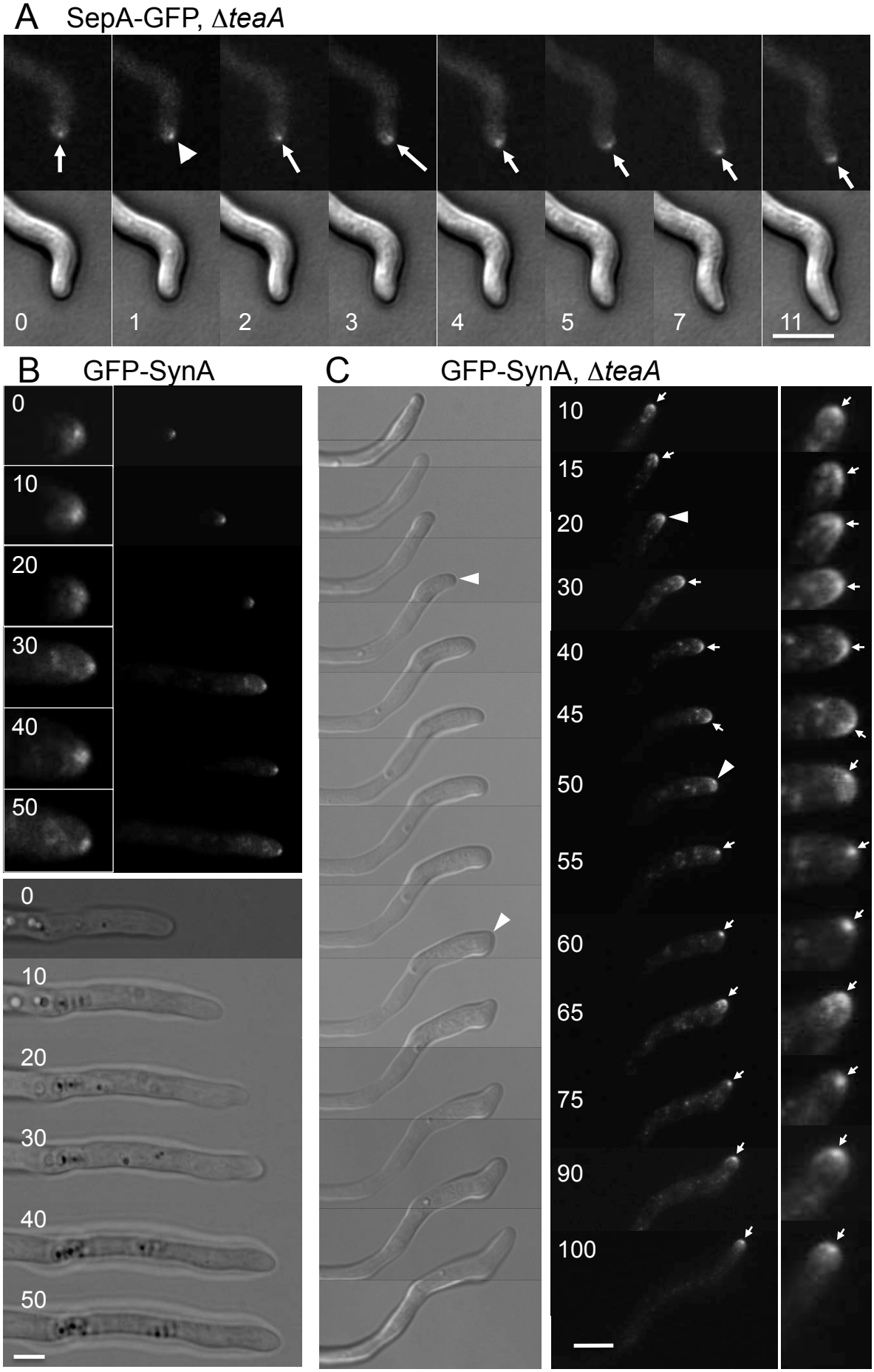
A SepA-GFP, ΔteaA
0
1
2
3
4
5
7
11
B GFP-SynA
0
10
20
30
40
50
0
10
20
30
40
50
C GFP-SynA, ΔteaA
10
15
20
30
40
45
50
55
60
65
75
90
100

Figure S2

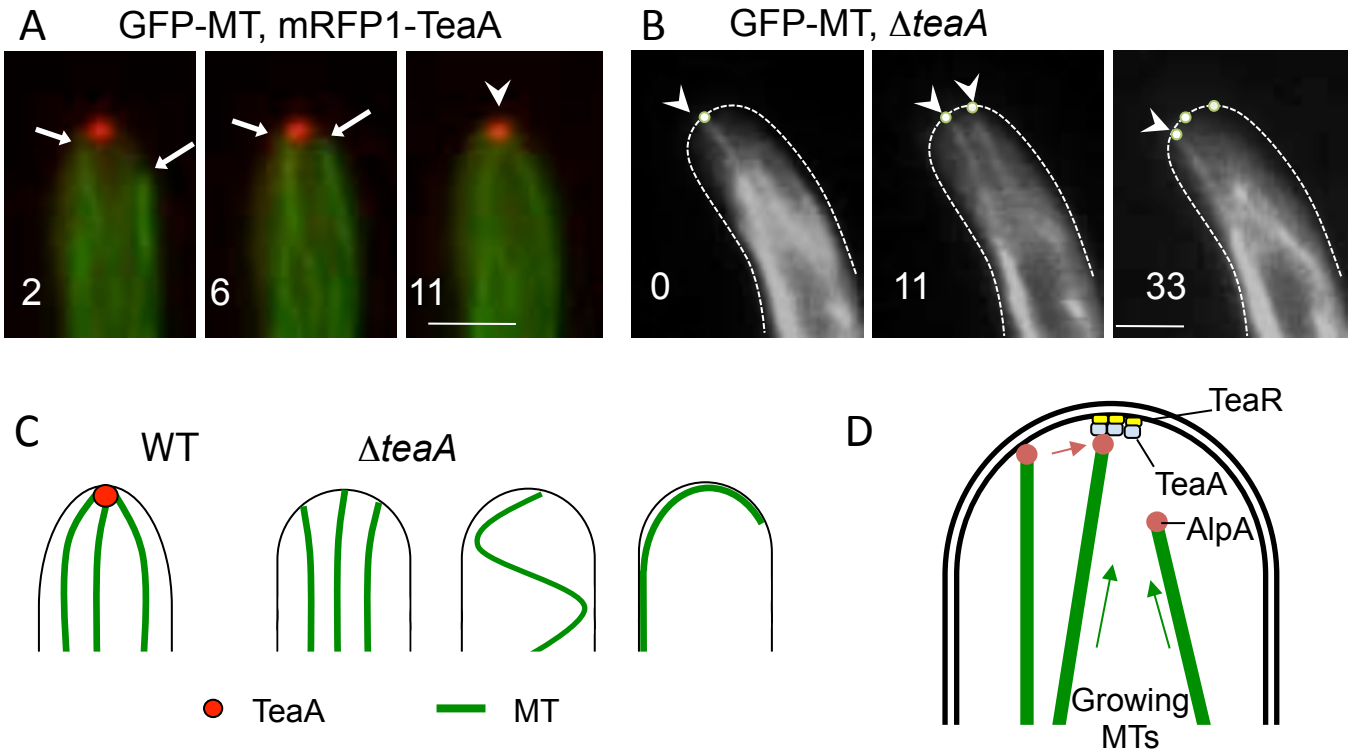
A
GFP-MT, mRFP1-TeaA
2
6
11
B
GFP-MT, ΔteaA
0
11
33
C
WT
ΔteaA
TeaA
MT
D
TeaR
TeaA
AlpA
Growing MTs
E
Membrane cortex
θ
Stop elongation
microtubule
Θ > α
Membrane cortex
θ'
Keep elongation
microtubule
Θ' < α
WT
ΔteaA
1.3 μm
X
X
WT
ΔteaA
F
MT
TeaA-TeaR
Growth machinery
SRD
Polarized growth
G
Polarity
Cell shape
MT growth

Figure S3

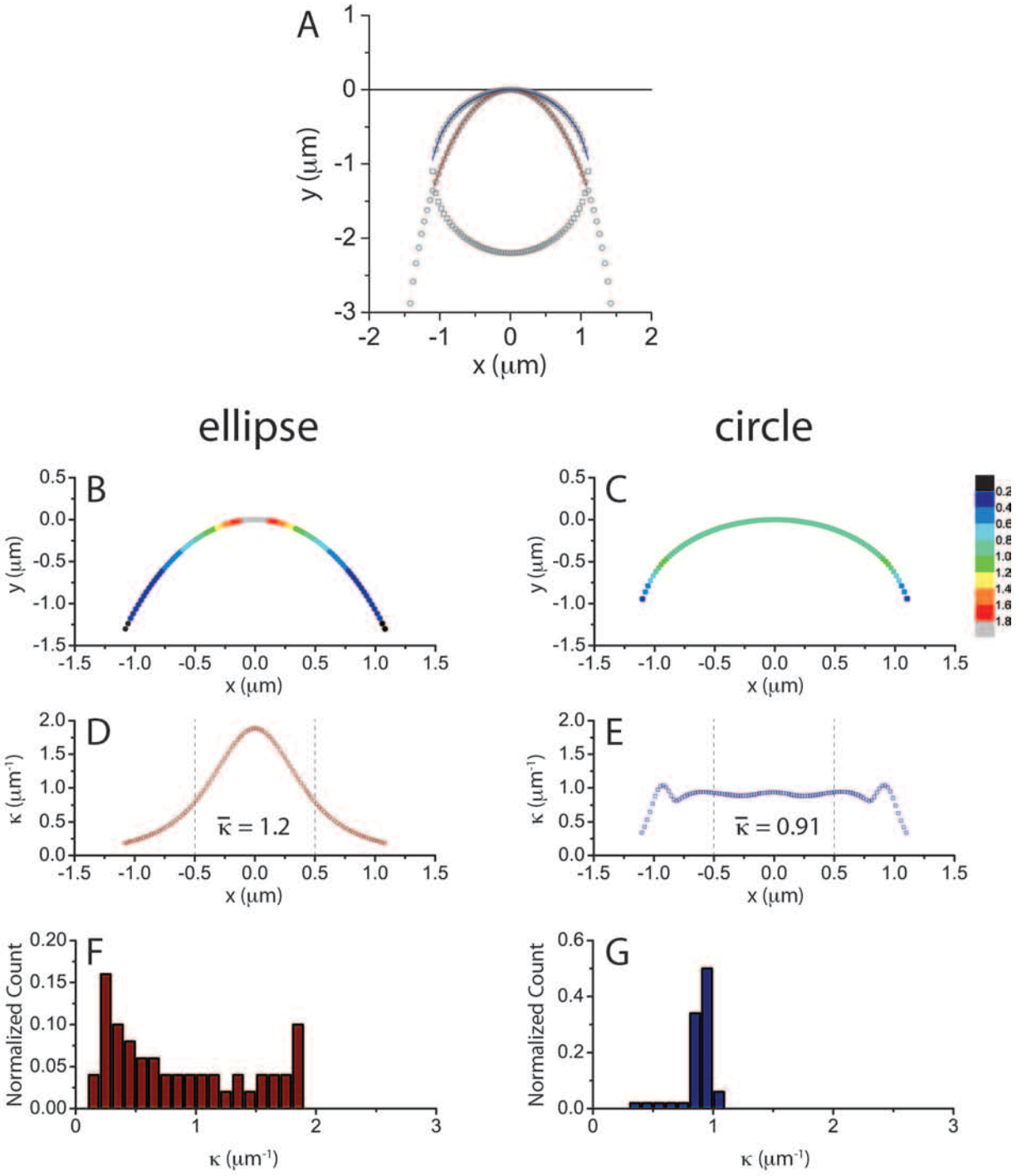
A
y (μm)
x (μm)
ellipse
circle
B
C
D
E
F
G
x (μm)
y (μm)
κ (μm⁻¹)
$\bar{\kappa}$ = 1.2
$\bar{\kappa}$ = 0.91
Normalized Count

Figure S4

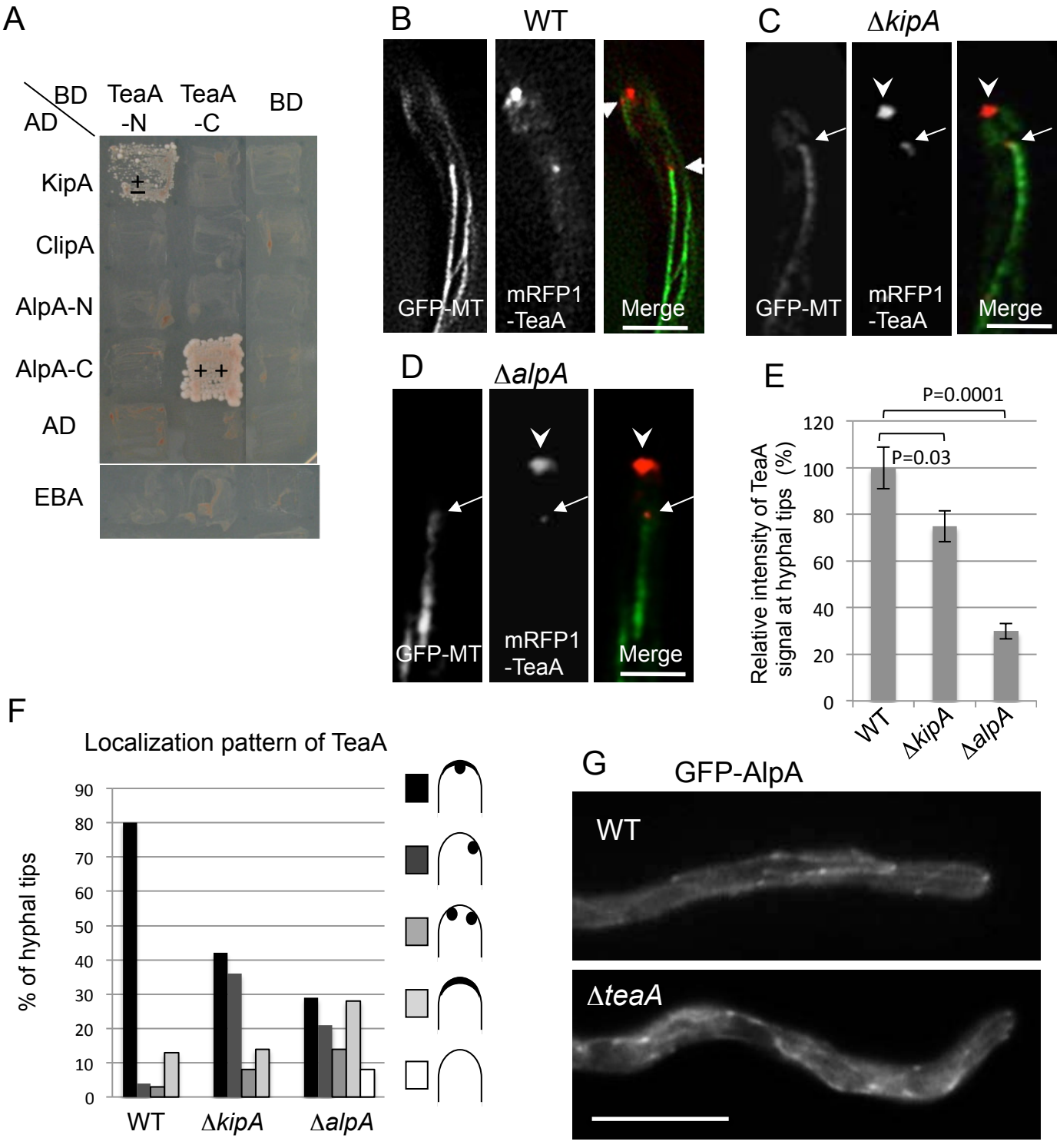
A
BD
AD
TeaA -N
TeaA -C
BD
KipA
ClipA
AlpA-N
AlpA-C
AD
EBA
±
+ +
B
WT
GFP-MT
mRFP1 -TeaA
Merge
C
ΔkipA
GFP-MT
mRFP1 -TeaA
Merge
D
ΔalpA
GFP-MT
mRFP1 -TeaA
Merge
E
P=0.0001
P=0.03
Relative intensity of TeaA signal at hyphal tips (%)
120
100
80
60
40
20
0
WT
ΔkipA
ΔalpA
F
Localization pattern of TeaA
% of hyphal tips
90
80
70
60
50
40
30
20
10
0
WT
ΔkipA
ΔalpA
G
GFP-AlpA
WT
ΔteaA

Figure S5

A

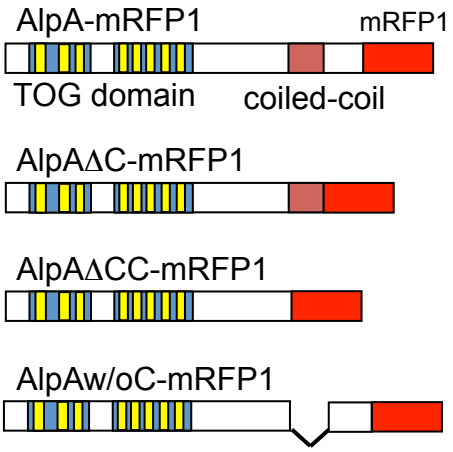

B

Localization	Number of MTs	Complementation of Δ*alpA*
MT, MT plus end	normal	+
MT (weak)	comparable	+
nucleus	few	–
nucleus	few	–

C

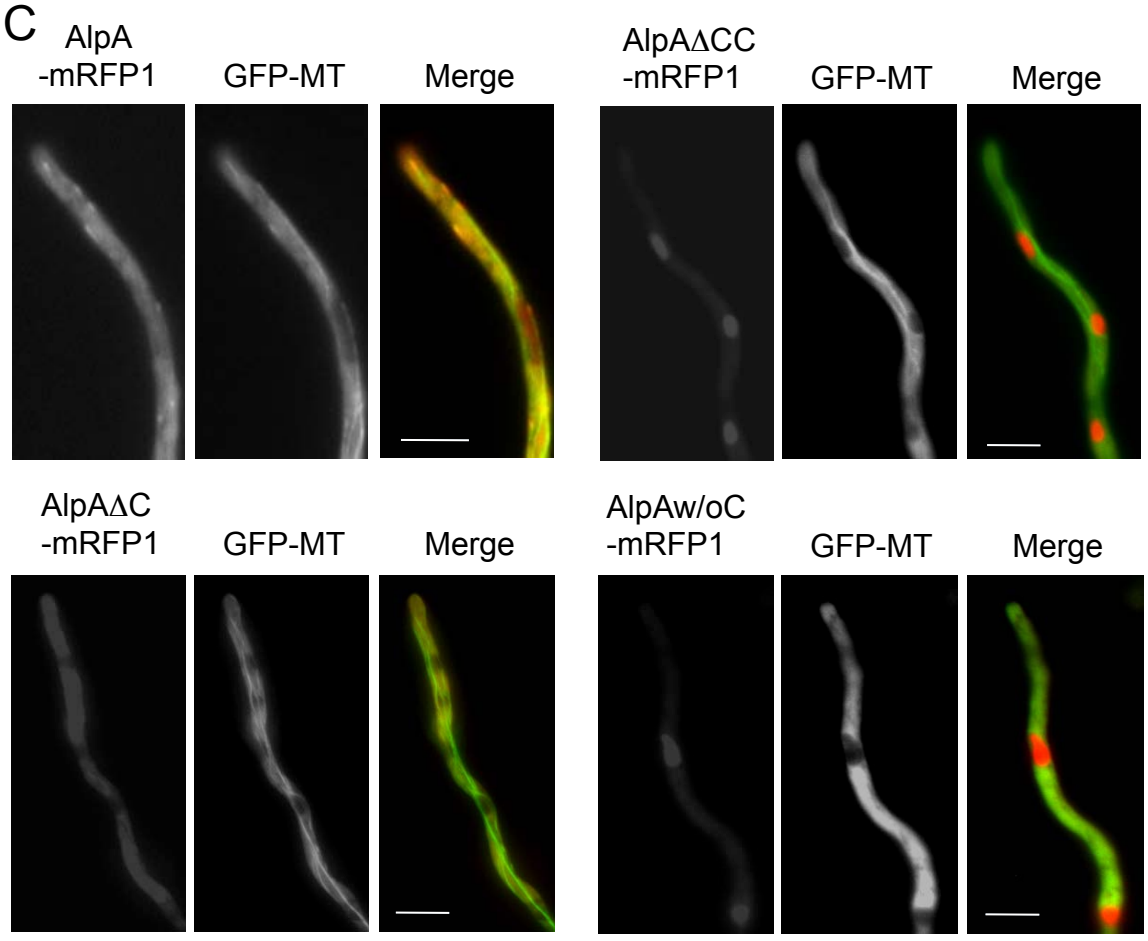

Figure S6

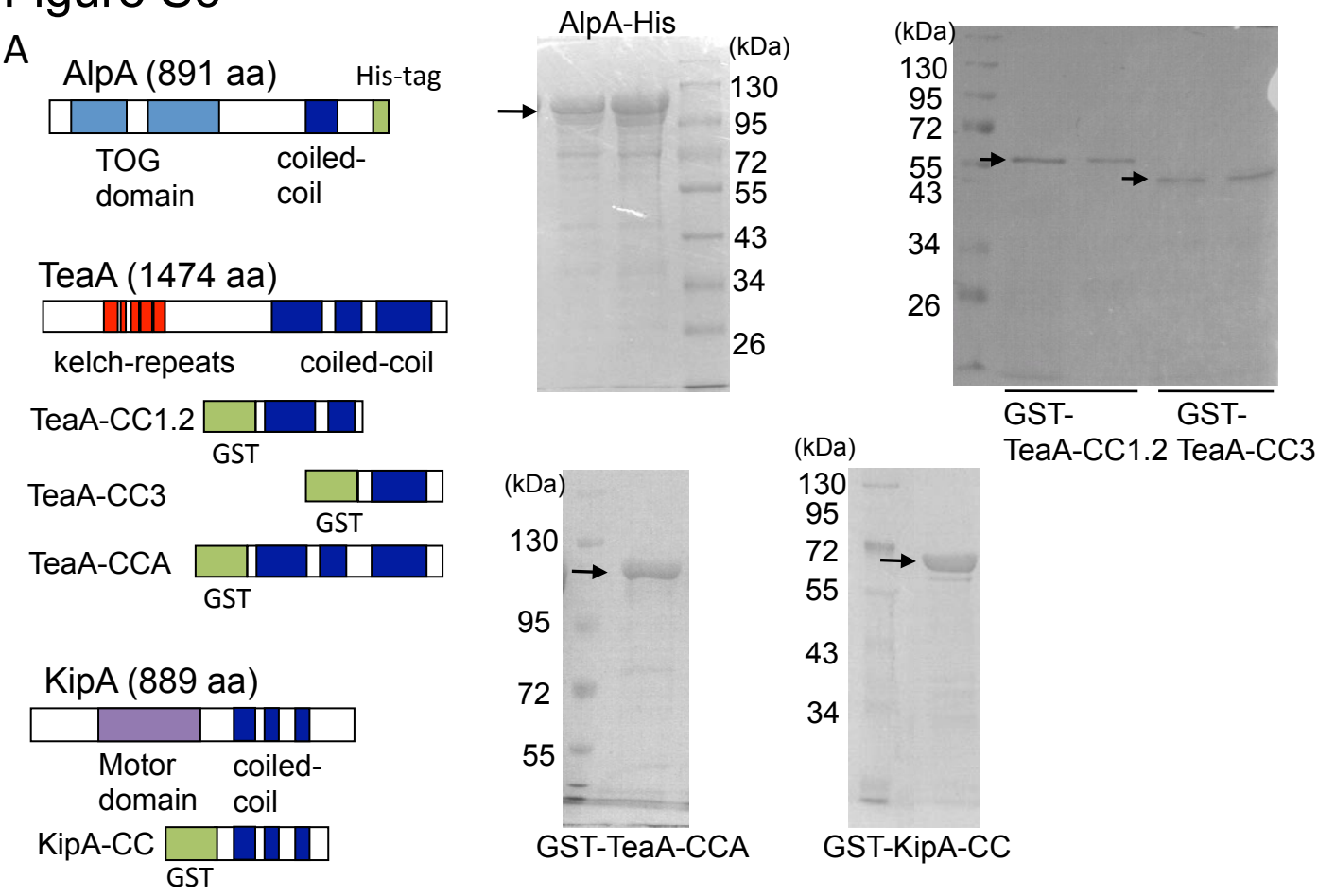
A
AlpA (891 aa)
His-tag
TOG domain
coiled-coil
TeaA (1474 aa)
kelch-repeats
coiled-coil
TeaA-CC1.2
GST
TeaA-CC3
GST
TeaA-CCA
GST
KipA (889 aa)
Motor domain
coiled-coil
KipA-CC
GST
AlpA-His
(kDa)
130
95
72
55
43
34
26
(kDa)
130
95
72
55
43
34
26
GST-TeaA-CC1.2
GST-TeaA-CC3
(kDa)
130
95
72
55
GST-TeaA-CCA
(kDa)
130
95
72
55
43
34
GST-KipA-CC

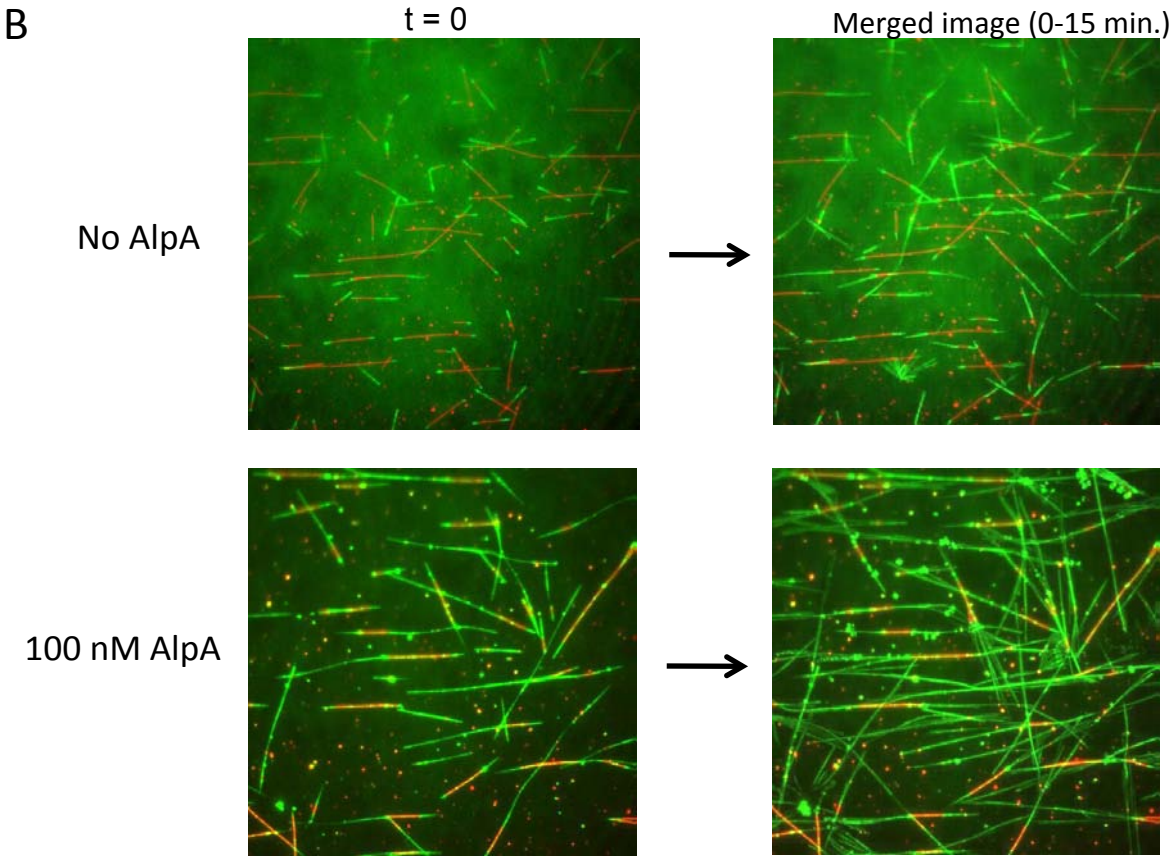
B
t = 0
Merged image (0-15 min.)
No AlpA
100 nM AlpA

Supplementary Materials

Figure S1. Localization of SepA-GFP and GFP-SynA. (A) The Δ*teaA* strain expressing GFP tagged SepA was grown in minimal medium at room temperature. Elapsed time is given in minutes, showing shorter interval time than Fig. 1. Scale bars represent 5 μm. (B, C) Wild type or Δ*teaA* strain expressing GFP tagged SynA were grown in minimal medium with glycerol at room temperature. At the hyphal tip of wild type, GFP-SynA localized to the spot at the apex (B). In contrast, at the tip of *teaA*-deletion strain, GFP-SynA localized to the spot at the apex but the spot often moved to side, which guided the growth direction (C). Elapsed time is given in minutes. Scale bars represent 2 μm.

Figure S2. Working model of microtubule guidance at the hyphal tip for polarity maintenance. (A) MTs elongated toward tips (arrows) and converged in one point at the apex where TeaA was concentrated (arrowhead). (B) GFP-MTs in the Δ*teaA* strain attached to several sites at the apex. Elapsed time is given in seconds. Scale bars represent 2 μm. (C) Summarized behavior of MTs at hyphal tip in the wild type and Δ*teaA* strain. (D) Scheme of interaction between TeaA at hyphal tip cortex and AlpA at MT plus ends. (E) Scheme indicating regulation of MT dynamics at the cortex depends on the angle of MTs and cortex. At the more round hyphal apex of Δ*teaA* strain, MT did not merged at apex and sometimes curled around the apical membrane. (F, G) Scheme of positive feedback loop by three-way deadlock.

Figure S3. The curvature distribution of an ellipse and a circle simulated tip. (A) In order to demonstrate how the shape influences the curvature distribution, hyphal tips have been approximated by an ellipse (open circle, similar to wild type hyphal tips) and a circle (open square, similar to Δ*teaA* hyphal tips) and subjected to the same curvature analysis. Solid lines represent the fitted spline curves. Local curvatures (κ, in μm^{-1}) of fitted spline curves are represented by color (B, C) and plotted along the x-axis (D, E). The difference in shape can easily be seen by the way the curvature changes along these approximated tips. The local curvature of the ellipsoidal shape continually increases as it approaches the tip of the ellipse, while the local curvature remains constant for the circle. The average κ in the region ± 0.5 μm is higher for the ellipse than for the circle. (F, G) The broadening of the local curvature distribution (for the entire *x* range) for the ellipse, in comparison to the circle, is another characteristic difference between two shapes.

Figure S4. TeaA and +TIPs. (A) Yeast two-hybrid analysis between TeaA (N-teminal half and C-terminal half) and +TIPs, KipA (C-terminal half, without motor domain), ClipA (Clip170 orthologue), AlpA (N-teminal half and C-terminal half) and EBA (AN2862, EB1 orthologue). The mated yeasts were grown on nutritionally selective plate SD/-Leu/-Trp/-His. (B-D) SNT65 (GFP-MTs, mRFP1-TeaA) (B, Data from Takeshita et al 2011), SNT76 (GFP-MTs, mRFP1-TeaA, Δ*kipA*) (C), SNT77 (GFP-MTs, mRFP1-TeaA, Δ*alpA*) (D) was grown in minimal medium with glycerol as carbon source. mRFP1-TeaA localized at hyphal tips (arrowheads) and at MT plus ends (arrows). The scale bars represent 5 μm. (E) Quantification of signal intensities of mRFP1-TeaA at tips in wild type, Δ*kipA*, Δ*alpA* strains. The whole tip apex was surrounded by a 2 μm - 1 μm rectangle, and the mean of signal intensity was measured by ImageJ. The data are expressed as the mean ± SEM, n = 20. Because the signal of mRFP1-TeaA at MT plus end was very weak, the brightness and contrast were differently adjusted in B-D. (F) The localization pattern of mRFP1-TeaA at 100 hyphal tips per strain was analyzed and grouped into five different categories. Each bar indicates the percentage of hyphal tips of these groups. (G) GFP-AlpA accumulated at MT plus ends and localized along MT filaments in the wild-type (upper) and Δ*teaA* strain (lower). The scale bars represent 10 μm. (Movie S3 and S4).

Figure S5. Functional analysis of truncated AlpA *in vivo*. Scheme of truncated AlpA versions. The results of the localization and function of truncated AlpA tagged with mRFP1 at the C-terminus are summarized in the table. AlpA-mRFP1 localized at MT plus ends and complemented the phenotype of a Δ*alpA* strain. AlpAΔC-mRFP1 localized along MTs and partially complemented the phenotype of a Δ*alpA* strain. AlpA without the coiled-coil region, AlpAΔCC-mRFP1 and AlpAw/oC-mRFP1, localized in nuclei and did not complemented the phenotype of a Δ*alpA* strain (slower growth and fewer MTs). The scale bars represent 5 μm.

Figure S6. (A) The His tagged AlpA, GST tagged TeaA C-terminal regions (TeaA-C1.2, TeaA-C3 and TeaA-CCA) and GST tagged KipA C-terminal region purified from *E. coli* were separated by SDS-PAGE and stained by coomassie staining. (B) MT polymerization assay in vitro. Images of a seed MT (red) with a

dynamic MT lattice growing from the plus end (green) at time = 0 (left) without AlpA (upper) and with 100 nM AlpA (lower). Merged images of total 15 min (right).

Supplementary Movies

Movie S1. GFP-KipA accumulation at MT plus ends moving toward hyphal tip and reaching one point at the apex. The GFP-KipA focus is constantly fed with new KipA from new MT plus ends reaching the focus.

Movie S2. GFP-KipA in a Δ*teaA* strain. In the *ΔteaA* strain individual MTs reach the cortex but are not meeting in the same focus at the tip. If one MT retracts then the signal disappears.

Movie S3. GFP-AlpA accumulated at MT plus ends and localized slightly along MT filaments in the wild-type.

Movie S4. GFP-AlpA accumulated at MT plus ends and localized slightly along MT filaments in the Δ*teaA* strain.

Movie S5. Dynamic behavior of MTs growth (green) from the stable MT seed (red) in the absence of AlpA. 10 s interval. Total 15 min.

Movie S6. Dynamic behavior of MTs growth (green) from the stable MT seed (red) in the presence of 100 nM AlpA. 10 s interval. Total 15 min.

Movie 1

Movie 2

Movie 3

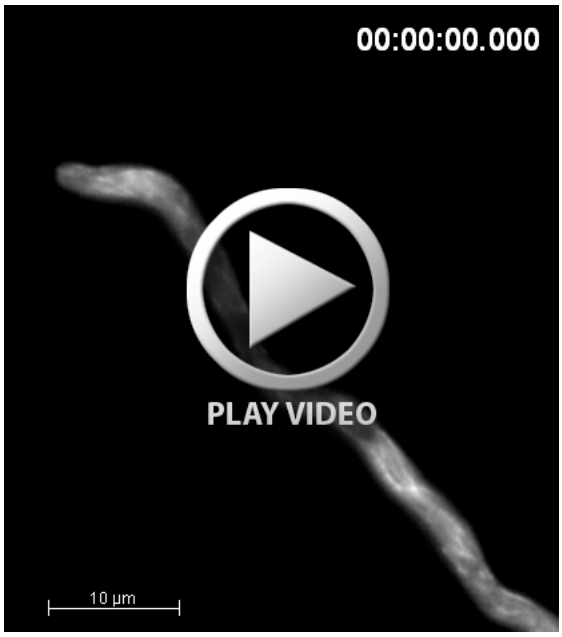

Movie 4

Movie 5

Movie 6

Table S1: *A. nidulans* strains used in this study

Strain	Genotype[a]	Source
TN02A3	*pyrG89; argB2; pyroA4; [ΔnkuA::argB]*	(Nayak, *et al*., 2006)
SRF200	*pyrG89; ΔargB::trpCΔB; pyroA4*	(Karos and Fischer, 1999)
AKS70	*pabaA1*; *pyrG89, [sepA::GFP::pyr-4]*	(Sharpless and Harris, 2002)
SNT30	*pyrG89; ΔargB::trpCΔB; pyroA4; [pyroA] [ΔteaA::argB]*	(Takeshita, *et al*., 2008)
SNT141	(AKS70 crossed to SNT30) *pyrG89, ΔargB::trpCΔB?; [sepA::GFP::pyr-4] ; [ΔteaA::argB]*	This study
SNG1	*pyrG89; argB2; ΔnkuA::argB; pyroA4; [alcA(p)-gfp-synA::pyr-4]*	This study
SNT126	(SNG1 crossed to SNT30) *pyrG89; argB2?; ΔnkuA::argB?; pyroA4?; [pyroA]; [alcA(p)-gfp-synA::pyr-4]; [ΔteaA::argB]*	This study
SJW02	*pyrG89; ΔargB::trpCΔB; pyroA4; [alcA(p)-gfp-tubA::pyr-4]*	J. Warmbold, Marburg, Germany
SNT65	*ΔargB::trpCΔB; [argB]; [alcA(p)-gfp-tubA::pyr-4] [teaA(p)-mrfp1-teaA::pyr-4]*	(Takeshita and Fischer, 2011)
SNT31	*pyrG89?; ΔargB::trpCΔB?; [alcA(p)-gfp-tubA::pyr-4]; [ΔteaA::argB]*	(Takeshita, *et al*., 2008)
SSK92	*pyrG89; pyroA4; [alcA(p)-gfp-kipA::pyr-4]*	(Konzack, *et al*., 2005)

SNT30	*pyrG89; ΔargB::trpCΔB; pyroA4; [pyroA]; [ΔteaA::argB]*	(Takeshita, *et al*., 2008)
SSK91	*pyrG89; ΔargB::trpCΔB; pyroA4; [ΔteaA::argB]*	(Takeshita, *et al*., 2008)
SNT10	*pyrG89; ΔargB::trpCΔB; pyroA4; [ΔteaA::argB]; [alcA(p)-gfp-kipA::pyr-4]*	This study
SSK44	*pabaA1; pyrG89?; ΔargB::trpCΔB; [ΔkipA::pyr-4]*	(Konzack, *et al*., 2005)
SSK67	*pabaA1; pyrG89?; [ΔkipA::pyr-4]; [alcA(p)-gfp-tubA::pyr-4]*	(Konzack, *et al*., 2005)
SNT52	*pabaA1; pyrG89?; ΔargB::trpCΔB; [teaA*(p)-mrfp1-*teaA*::*pyr-4]*	(Takeshita, *et al*., 2008)
SNT76	(SSK67 crossed to SNT52) *pyrG89?; [ΔkipA::pyr-4]; [alcA(p)-gfp-tubA::pyr-4]; [teaA*(p)-mrfp1-*teaA*::*pyr-4]*	This study
SDV86	*pabaA1; pyrG89?; [alcA(p)-gfp-tubA::pyr-4]; [ΔalpA::pyr-4]*	(Enke, *et al*., 2007)
SNT77	(SDV86 crossed to SNT52) *pyrG89?; [alcA(p)-gfp-tubA::pyr-4]; [ΔalpA::pyr-4]; [teaA*(p)-mrfp1-*teaA*::*pyr-4]*	This study
SNT49	*pyrG89; argB2; pyroA4; [ΔnkuA::argB]; [teaA*(p)-mrfp1-*teaA*::*pyr-4]*	(Takeshita, *et al*., 2008)
SNT50	*pyrG89?; argB2?; ΔargB::trpCΔB?; [ΔnkuA::argB]; [teaA*(p)-mrfp1-*teaA*::*pyr-4]; [ΔkipA::pyr-4]*	(Takeshita, *et al*., 2008)
SCS13a	*pyrG89; argB2; pyroA4; [ΔnkuA::argB]; [ΔalpA::pyr-4]*	(Enke, *et al*., 2007)
SNT69	(SCS13a crossed to SNT52) *pyrG89?; argB2?; ΔargB::trpCΔB?; [ΔnkuA::argB]; [ΔalpA::pyr-4]; [teaA*(p)-	This study

	mrfp1-*teaA*::*pyr-4]*	
SCE05	*pyrG89; ΔargB::trpCΔB; pyroA4; [alcA(p)-gfp-alpA::pyr-4]*	(Enke, *et al*., 2007)
SNT72	(SCE05 cross to SNT30) *pyrG89; ΔargB::trpCΔB; pyroA4; [pyroA]; [alcA(p)-gfp-alpA::pyr-4]; [ΔteaA::argB]*	This study
SSH62	*pyrG89; argB2; pyroA4; [ΔnkuA::argB]; [alcA(p)-mcherry-tubA::pyr-4]*	This study
SNT71	(SCE05 crossed to SNT52) *pyrG89?; ΔargB::trpCΔB; [alcA(p)-gfp-alpA::pyr-4]; [teaA*(p)-mrfp1-*teaA*::*pyr-4]*	This study
SNT100	(SSH62 crossed to SNT71) *pyrG89?; argB2?; ΔargB::trpCΔB?; [ΔnkuA::argB]; [alcA(p)-gfp-alpA::pyr-4]; [alcA(p)-mcherry-tubA::pyr-4]*	This study
SYH07	*pyrG89; argB2; pyroA4; [ΔnkuA::argB]; [alcA*(p)-*yfp*^{N}-*teaA::pyr-4]; [alcA*(p)-*yfp*^{C}-*alpA::pyr-4]*	This study
SYH35	*pyrG89; argB2; pyroA4; [ΔnkuA::argB]; [teaA*(p)-*yfp*^{N}-*teaA::pyr-4]; [alcA*(p)-*yfp*^{C}-*alpA::pyr-4]*	This study
SMD04	*pabaA1; pyrG89?; [pabaA]; [alcA(p)-gfp-tubA::pyr-4]; [ΔalpA::pyr-4] [alcA(p)-alpA-mrfp1::argB]*	This study
SMD02	*pabaA1; pyrG89?; [pabaA]; [alcA(p)-gfp-tubA::pyr-4]; [ΔalpA::pyr-4] [alcA(p)-alpA*ΔC-*mrfp1::argB]*	This study
SMD01	*pabaA1; pyrG89?; [pabaA]; [alcA(p)-gfp-tubA::pyr-4]; [ΔalpA::pyr-4] [alcA(p)-alpA*ΔCC-*mrfp1::argB]*	This study
SMD03	*pabaA1; pyrG89?; [pabaA]; [alcA(p)-gfp-tubA::pyr-4]; [ΔalpA::pyr-4] [alcA(p)-alpAw/o*C-*mrfp1::argB]*	This study
SNT80	(SSK91 crossed to SJW02) *pyrG89; ΔargB::trpCΔB; pyroA4;*	This study

	[alcA(p)-gfp-alpA::pyr-4]; [ΔteaA::argB]	
SNT92	*pyrG89; ΔargB::trpCΔB; pyroA4; [pyroA]; [alcA(p)-gfp-alpA::pyr-4]; [ΔteaA::argB]; [alcA(p)-teaA-mrfp1::argB]*	This study
SNT86	*pyrG89; ΔargB::trpCΔB; pyroA4; [pyroA]; [alcA(p)-gfp-alpA::pyr-4]; [ΔteaA::argB]; [alcA(p)-teaA*ΔCC3-*mrfp1::argB]*	This study
SNT87	*pyrG89; ΔargB::trpCΔB; pyroA4; [pyroA]; [alcA(p)-gfp-alpA::pyr-4]; [ΔteaA::argB]; [alcA(p)-teaA*ΔCC-*mrfp1::argB]*	This study
SNT88	*pyrG89; ΔargB::trpCΔB; pyroA4; [pyroA]; [alcA(p)-gfp-alpA::pyr-4]; [ΔteaA::argB]; [alcA(p)-teaA*ΔCC1.2-*mrfp1::argB]*	This study
SNT93	*pyrG89; ΔargB::trpCΔB; pyroA4; [pyroA]; [alcA(p)-gfp-alpA::pyr-4]; [ΔteaA::argB]; [teaA(p)-teaA*ΔCC3-*mrfp1::argB]*	This study
SNT89	*pyrG89; ΔargB::trpCΔB; pyroA4; [ΔteaA::argB]; [alcA*(p)-*yfp^N-teaA*ΔCC3*::pyr-4]; [alcA*(p)-*yfp^C-alpA::pyr-4]*	This study
SNT90	*pyrG89; ΔargB::trpCΔB; pyroA4; [ΔteaA::argB]; [alcA*(p)-*yfp^N-teaA*ΔCC*::pyr-4]; [alcA*(p)-*yfp^C-alpA::pyr-4]*	This study
SNT91	*pyrG89; ΔargB::trpCΔB; pyroA4; [ΔteaA::argB]; [alcA*(p)-*yfp^N-teaA*ΔCC1.2*::pyr-4]; [alcA*(p)-*yfp^C-alpA::pyr-4]*	This study

[a] All strains harbour in addition the *veA1* mutation. *wA3* and *yA2 are not shown*.

Table S2: Plasmids used in this study

Plasmids	Construction	Source
pCR2.1-TOPO	Cloning vector	Invitrogen (NV Leek, The Netherlands)
pENTR/D-TOPO	Entry vector in gateway system	Invitrogen (NV Leek, The Netherlands)
pMT-mRFP1	Destination vector for mRFP1 tagging at C-terminus, expression under *alcA* promoter in gateway system	(Toews, et al., 2004)
pET101/D-TOPO	*E. coli* expression vector, T7 promoter, His-tag	Invitrogen (NV Leek, The Netherlands)
pET28a	*E. coli* expression vector, T7 promoter, His-tag, S-tag	Novagen
pCMB17apx	*alcA(p)::GFP*, for N-terminal fusion of GFP to proteins of interest; contains *N. crassa pyr-4*	V. Efimov (Piscataway, USA)
pSK82	1-kb *kipA* fragment in pCMB17apx	(Konzack, *et al*., 2005)
pDV7	GFP replaced N-terminal half of YFP in pCMB17apx	(Takeshita *et al*. 2008)
pDV8	GFP replaced C-terminal half of YFP in pCMB17apx	(Takeshita *et al*. 2008)
pYH01	0.7-kb *teaA* fragment from pNT1 in pDV7	(Takeshita *et al*. 2008)
pYH12	N-terminal 1.0-kb *alpA* fragment in pDV8	This study
pNT28	*teaA(p)::mRFP1::TeaA::pyr-4*	(Takeshita *et al*. 2008)
pNT34	N-terminal half of *teaA* (1-674 aa) cDNA in pGBKT7	(Takeshita *et al*. 2008)
pSH19	C-terminal half of *teaA* (661-1474 aa) cDNA in pGBKT7	(Takeshita *et al*. 2008)
pSH09	*kipA* C-terminal (505-889 aa) cDNA in pGADT7	(Herrero *et al*. 2011)

pYH20	*clipA* cDNA in pGADT7	This study
pSH08	*kipA* C-terminal (505-889 aa) cDNA in pGBKT7	(Herrero *et al*. 2011)
pYH26	*clipA* cDNA in pGBKT7	This study
pNT37	N-terminal half of *alpA* (1-414 aa) cDNA in pGADT7	This study
pYH22	C-terminal half of *alpA* (AlpA-C, 414-892 aa) cDNA in pGADT7	This study
pYH25	C-terminal half of *alpA* (AlpA-C, 414-892 aa) cDNA in pGBKT7	This study
pCE07	*alcA(p)::alpA::3xHA::argB*; gateway construct	This study
pDM06	C-terminal half of AlpA without C-terminal region (AlpA-ΔC, 414-756 aa) cDNA in pGADT7	This study
pDM07	C-terminal half of AlpA without C-terminal and coiled-coil region (AlpA-ΔCC, 414-644 aa) cDNA in pGADT7	This study
pDM08	C-terminal half of AlpA without C-terminal region (AlpA-ΔC, 414-756 aa) cDNA in pGBKT7	This study
pDM09	C-terminal half of AlpA without C-terminal and coiled- coil region (AlpA-ΔCC, 414-644 aa) cDNA in pGBKT7	This study
pNT39	C-terminal region of *teaA* (TeaA-C1.2, 1011-1117 aa) cDNA in pGBKT7	This study
pNT40	C-terminal region of *teaA* (TeaA-C3, 1133-1474 aa) cDNA in pGBKT7	This study
pMD04	*alcA(p)::alpA::mRFP1::argB*; gateway construct	This study
pMD02	*alcA(p)::alpA*ΔC*::mRFP1::argB*; gateway construct	This study

pMD01	*alcA(p)::alpA*ΔCC*::mRFP1::argB*; gateway construct	This study
pMD03	*alcA(p)::alpAw/oC::mRFP1::argB*; gateway construct	This study
pDM05	*alcA(p)::mRFP1::argB*; gateway construct	This study
pNT19	*alcA(p)::teaA::mRFP1::argB*; gateway construct	This study
pNT41	*alcA(p)::teaA*ΔC2*::mRFP1::argB*; gateway construct	This study
pNT42	*alcA(p)::teaA*ΔC*::mRFP1::argB*; gateway construct	This study
pNT43	*alcA(p)::teaA*ΔC1*::mRFP1::argB*; gateway construct	This study
pNT44	*alcA(p)::YFP^N::TeaA*Δ*C1::pyr-4*	This study
pNT45	*alcA(p)::YFP^N::TeaA*Δ*C::pyr-4*	This study
pNT46	*alcA(p)::YFP^N::TeaA*Δ*C2::pyr-4*	This study
pNT50	*teaA(p)::mRFP1::TeaA*Δ*C2::pyr-4*	This study
pNT53	C-terminal region of *teaA* (TeaA-C1.2, 661-1122 aa) cDNA in pGEX-4T-1	This study
pNT54	C-terminal region of *teaA* (TeaA-C3, 1061-1474 aa) cDNA in pGEX-4T-1	This study
pNT74	C-terminal region of *teaA* (TeaA-CA, 661-1474 aa) cDNA in pGEX-4T-1	This study
pNT73	coiled-coil region of KipA (KipA-CC)(505-800 aa) cDNA in pGEX-4T-1	This study
pNT49	Codon optimized full-length of *alpA* cDNA in pET28a	This study
pNG2	*synA* fragment in pCMB17apx	This study

Table S3: Primers used in this study

ClipA-F-SMARTIII	5'-AAGCAGTGGTATCAACGCAGAGTGGATGGCGCCTCTGGACGA-3'
ClipA-R-CDSIII	5'-TCTAGAGGCCGAGGCGGCCGACATGTTAATCATCGAACGGGCAG-3'
AlpA-F-EcoRI	5'-GGCCGAATTCATGCCTGAAGGAGAGGAAG-3'
AlpA-N,CDSIII	5'-GCCGAGGCGGCCGACATGAGGGCGGTGCTTGACGAA-3'
AlpA-MEF	5'-GAATTCACGGTCATGCCACCGATC-3'
AlpA-R-BamHI	5'-GGCCGGATCCTTAGCGTTGGGCTGGTTG-3'
AlpA-CC-BamHI-rev	5'-GGATCCAAACTGATCAGGAATAGCAGTTGG-3'
AlpA-bCC-BamHI-rev	5'-GGATCCGTCCACTCACAGCAGGAGCGG-3'
TeaA,C,1,F,pGBK	5'-GGCGAATTCCCTCGCTCACCACGGTTG-3'
TeaA,C,1,R,pGBK	5'-GGCGGATCCGGCGTCTACTATCCGTGTAAC-3'
TeaA,C,3,F,pGBK	5'-GGCGAATTCTATCAGGAGCAGGCTAGTAGG-3'
TeaA,C,3,R,pGBK	5'-GGCGGATCCCGATCATATTCGCTGCCGCTT-3'
alpA-pENTR-fwd	5'-CACCATGCCTGAAGGAGAGGAAGA-3'
alpA-pENTR-rev	5'-GCGTTGGGCTGGTTGT-3'
alpA-CC-rev	5'-AAACTGATCAGGAATAGCAGTTGG-3'
alpA-bCC-AscI-rev	5'-GGCGCGCCGTCCACTCACAGCAGGAGCGG-3'
alpA-Ct-AscI-fwd	5'-GGCGCGCCATGAGTTCTCCAACTGCTATTC-3'
alpA-Ct-AscI-rev	5'-GGCGCGCCTGCGTTGGGCTGGTTGTC-3'
teaA-N-for	5'- CACCATGGCGGGTACAGCTAC-3'
TeaA-C1-rev	5'-TCTACTATCCGTGTAAC-3'
teaA-C-rev-smaI	5'-CCCGGGAAACAAGGCCTCCTGGTG-3'
teaA-C2-f-smaI	5'-CCCGGGTATCAGGAGCAGGCTAGTAG-3'
teaA-C2-rev-smaI	5'-CCCGGGGATCATATTCGCTGCCGCTT-3'
BiFC-teaA-f-psiI	5'-TTATAAACCCGGTGTCCAAA-3'
BiFC-teaA-N-rev-pacI	5'-TTAATTAAAACAAGGCCTCCTGGTG-3'
BiFC-teaA-C1-rev-pacI	5'-TTAATTAATTAGCGTCTACTATCCGTGTA-3'
BiFC-teaA-C2-re-pacI	5'-TTAATTAATTAGATCATATTCGCTGCCGC-3'

GST-TeaAC1-f-bam	5'-GGATCCCCTCGCTCACCACGGTTGAC-3'
GST-TeaAC1-r-eco	5'-GAATTCGCGTCTACTATCCGTGTAAC-3'
GST-TeaAC3-f-bam	5'-GGATCCTATCAGGAGCAGGCTAGTAGG-3'
GST-TeaAC3-r-eco	5'-GAATTCGATCATATTCGCTGCCGCTT-3'
SynA_AscI_fwd	5'-CGGCGCGCCTATGTCTGAGCAACCGTAC-3'
PacI_SynA_rev2	5'-CCTTAATTAATCAGCGCATAGTATCGACGGTC-3'
KipCC-GST-f-BmH	5'-GCGGGATCCTCGCTGGTCAGTATTCTTTG-3'
kipCC-GST-r-Xho	5'-GCGCTCGAGTATCCAATGTGAGCTGGGCAA-3'

References in Supplementary Materials

Herrero S, Takeshita N, Fischer R. (2011). The *Aspergillus nidulans* CENP-E kinesin motor KipA interacts with the fungal homologue of the centromere-associated protein CENP-H at the kinetochore. *Mol. Microbiol.* 80, 981-94.

Karos M, Fischer R. (1999). Molecular characterization of HymA, an evolutionarily highly conserved and highly expressed protein of *Aspergillus nidulans*. *Mol. Gen.Genet.* 260, 510-21.

Nayak T, Szewczyk E, Oakley CE, Osmani A, Ukil L, Murray SL, Hynes MJ, Osmani SA, Oakley BR. (2006). A versatile and efficient gene-targeting system for *Aspergillus nidulans*. *Genetics* 172, 1557-66.

Toews MW, Warmbold J, Konzack S, Rischitor P, Veith D, Vienken K, Vinuesa C, Wei H, Fischer R. (2004). Establishment of mRFP1 as a fluorescent marker in *Aspergillus nidulans* and construction of expression vectors for high-throughput protein tagging using recombination in vitro (GATEWAY). *Curr. Genet.* 45, 383-9.